nature ecology & evolution

Article

https://doi.org/10.1038/s41559-023-02165-y

Species-wide genomics of kākāpō provides tools to accelerate recovery

In the format provided by the authors and unedited

Supplemental

Te Reo Abstract

He kākā whakamōrea tata korehāhā, ao āta whakahaere te kākāpō nō Aotearoa. Kei te takiwā o te 200 manu e ora tonu ana. E tātari nei mātou i te raraunga huinga-ira katoa ki te rahinga o ngā kākāpō kia whakaputa mai ai he raraunga SNP whai kounga mō te katoa o tēnei momo manu. Ka whakamahia e mātou he raraungameta kōrahi karioi ki te ine rahi i te kanorau o te toenga o te kōrero ira o tēnei momo kākā, ā, ka whakaritea he ara ki te whakatūhono i te pītau ira ahurei ki te whakatinanatanga o tōna pītau ira mā te momo tātari e hāngai ana ki ngā kararehe taupori paku. Kua whakaatuhia ā mātou tātaritanga, mā te whakahaerenga o te whakauka kua mau pūmau te kanorau ira o te taupori nei. Ka whakaatuhia hoki ētahi ara hou e whakamahia ana i te ara whakahaere matapae pāpono mā te whakamahi hoki i tētahi anga ako pūrere me te huinga raraunga āhua pītau ira e tūhāngai ana ki te rima ngahuru tau, ki te wāwāhi i ngā āhua rerenga ki ngā pānga taiao me ngā pānga ira i a mātou e ine tonu ana i te warawara o ā mātou whakatau tata. Ka kitea te hononga o te whakatupu, o te rahi o te punipuni, o te whakaraerae ki te tahumaero, ā, o te matahua hoki o ngā hua ki ngā rohenga ira kua whakaatu kē tō rātou awenga ki ēnei huaira ki momo kē, e whakaatuhia ana ngā hua maha ka puta i te aro o tā mātou mahi. Nā reira, ka puta atu mātou he tikanga whakatupu kia matapae ai te āhua pītau ira, ā, ka whakaatu hoki ko te āta poipoi te take i mau pūmau ai te kanorau i roto i ngā tikanga whakatupu, waihoki, ko te pitomata o whanake whakamua. Ka rato hoki mātou he ara mō ngā whakatau whakahaere e haere ake nei, ko te kaitiakitanga hoki, tae noa atu ki te tūtohu i ngā manu ka nuku atu ki wāhi kē atu, me te āta mātai i ngā manu pōnīnī, i ngā manu mōrea nui ki te tahumaero. Hei whakakapinga, he mea arataki tēnei rangahau ki te whakamahi i te pītau ira ahurei mātotoru me ngā hua maha o te āta atawhai i ēnei manu.

The Te Reo Māori version of the Abstract is published as supplied by the authors.

DeepVariant Training

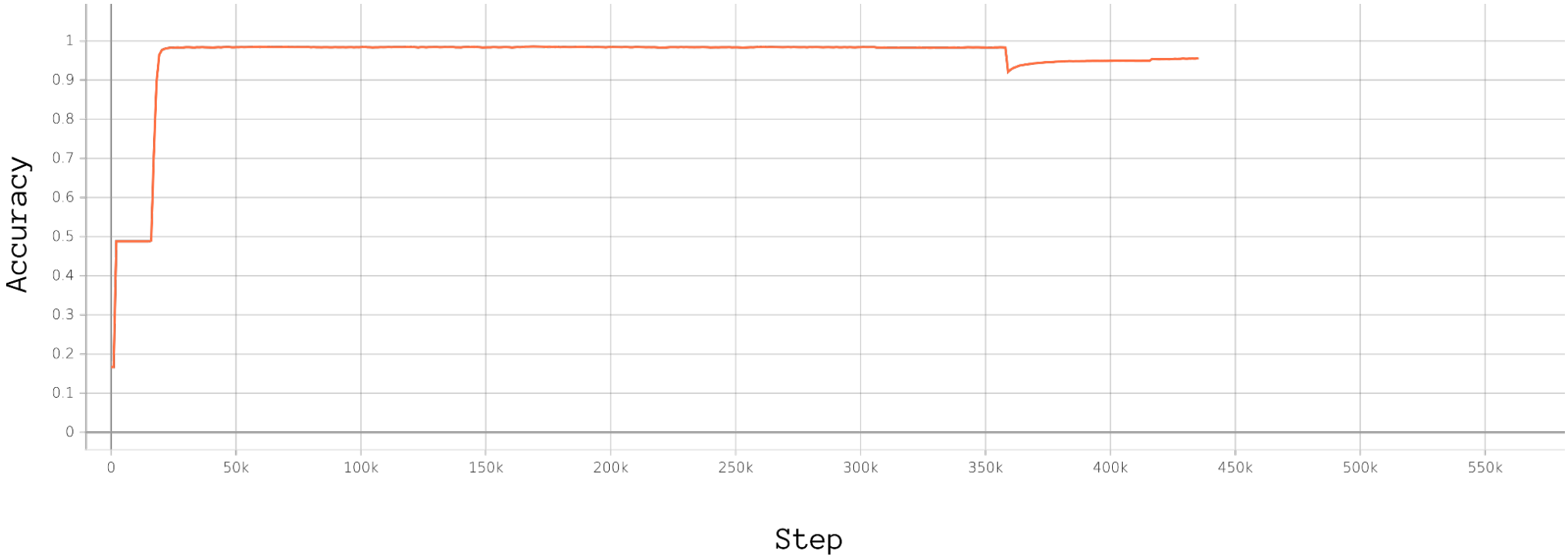

Supplementary Figure 1. Accuracy of SNPs and indels across training batches for a trained DeepVariant model for kākāpō. The training was interrupted near 360k, and the downsampling was altered to improve SNP calling in low-coverage regions. See main text for details.

Variant Calling Models

In total, three variant calling pipelines were tested, DeepVariant, which produced the final variant call, FreeBayes v1.2.0-dirty, and GATK 4.1.4.1. Initial quality checks for Mendelian inheritance error and genotype quality scores determined that FreeBayes performance was much lower than for DeepVariant and GATK, and so results from this pipeline were not used further. GATK was used to individually call variants on the full-read set. GATK genomic VCFs, which include statistics for each genomic position, were joint-called and combined using GLNexus; results were comparable but had a higher Mendelian inheritance error rate (3.38%) than DeepVariant (1.28%, Supplementary Figure 2).

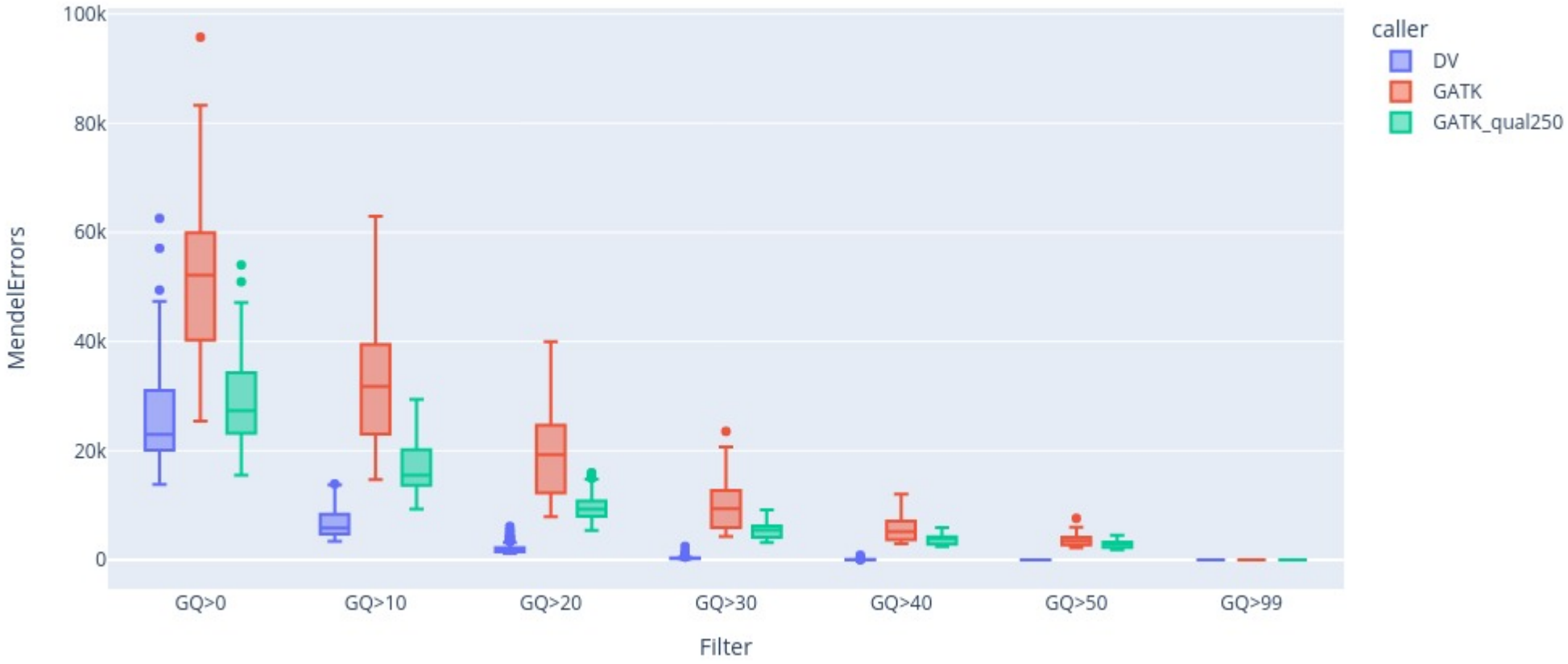

Supplementary Figure 2. Mendelian inheritance errors for identified variants were categorized by genotype quality (GQ) to compare our trained DeepVariant model for kākāpō with GATK and GATK filtering on QUAL scores >= 250. MendelErrors are errors in the offspring with n=122 confirmed Trios. DeepVariant contained 2,501,211 variants (SNPs, indels, others) after filtering, while GATK and GATK250 contained 4,047,873 and 2,419,722,

respectively. The median error rate is marked as a line inside the box, and the ends of the boxes represent the lower and upper quartiles. Fences are defined as their respective quartile +/- 1.5 times the inter quartile range. Data outside of the fences are plotted individually.

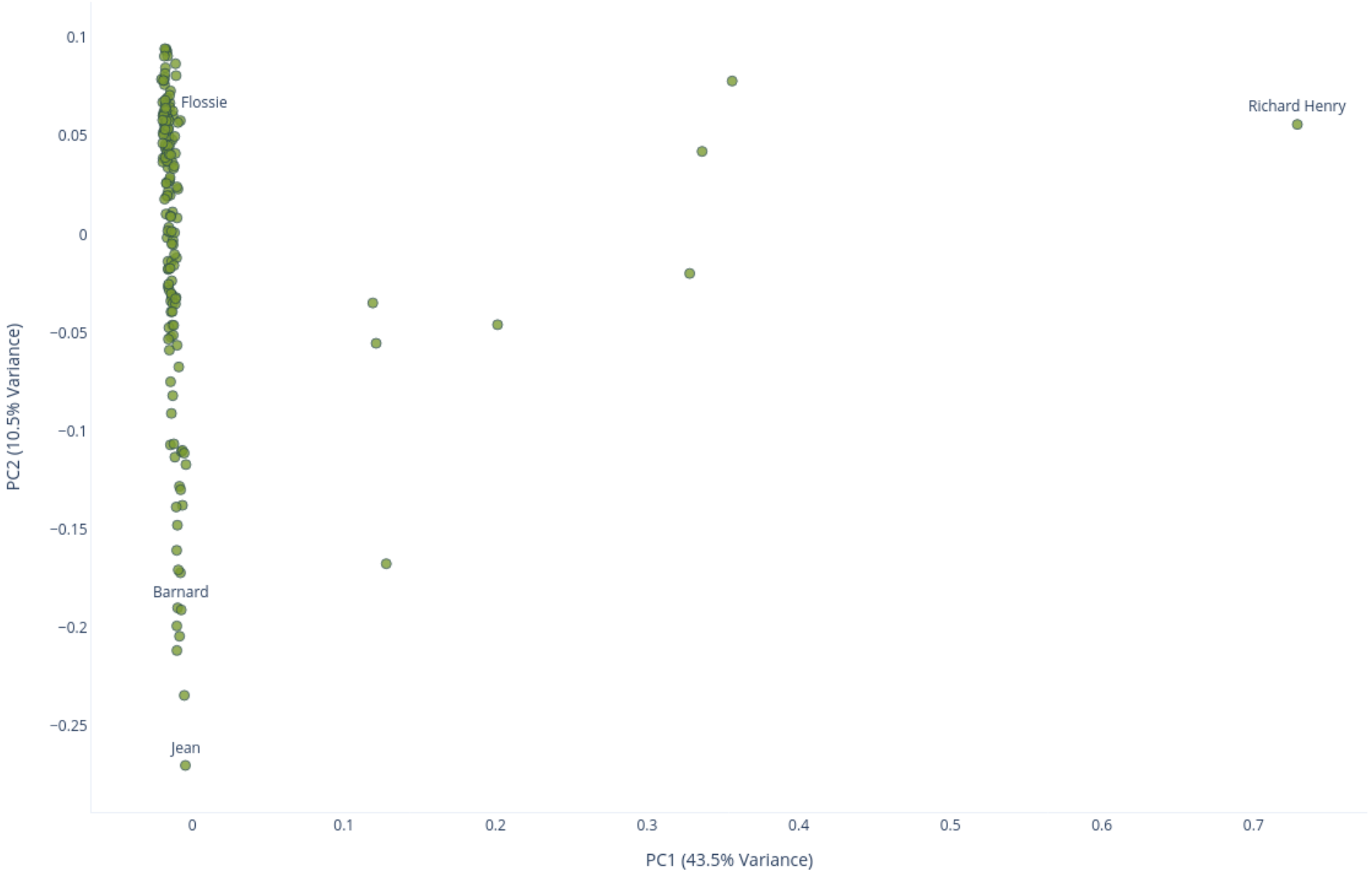

Supplementary Figure 3. PCA of Our Population. Population PCA determined from biallelic SNPs with fewer than 20% missing allele calls and SNP quality >= 99. Half calls set to missing.

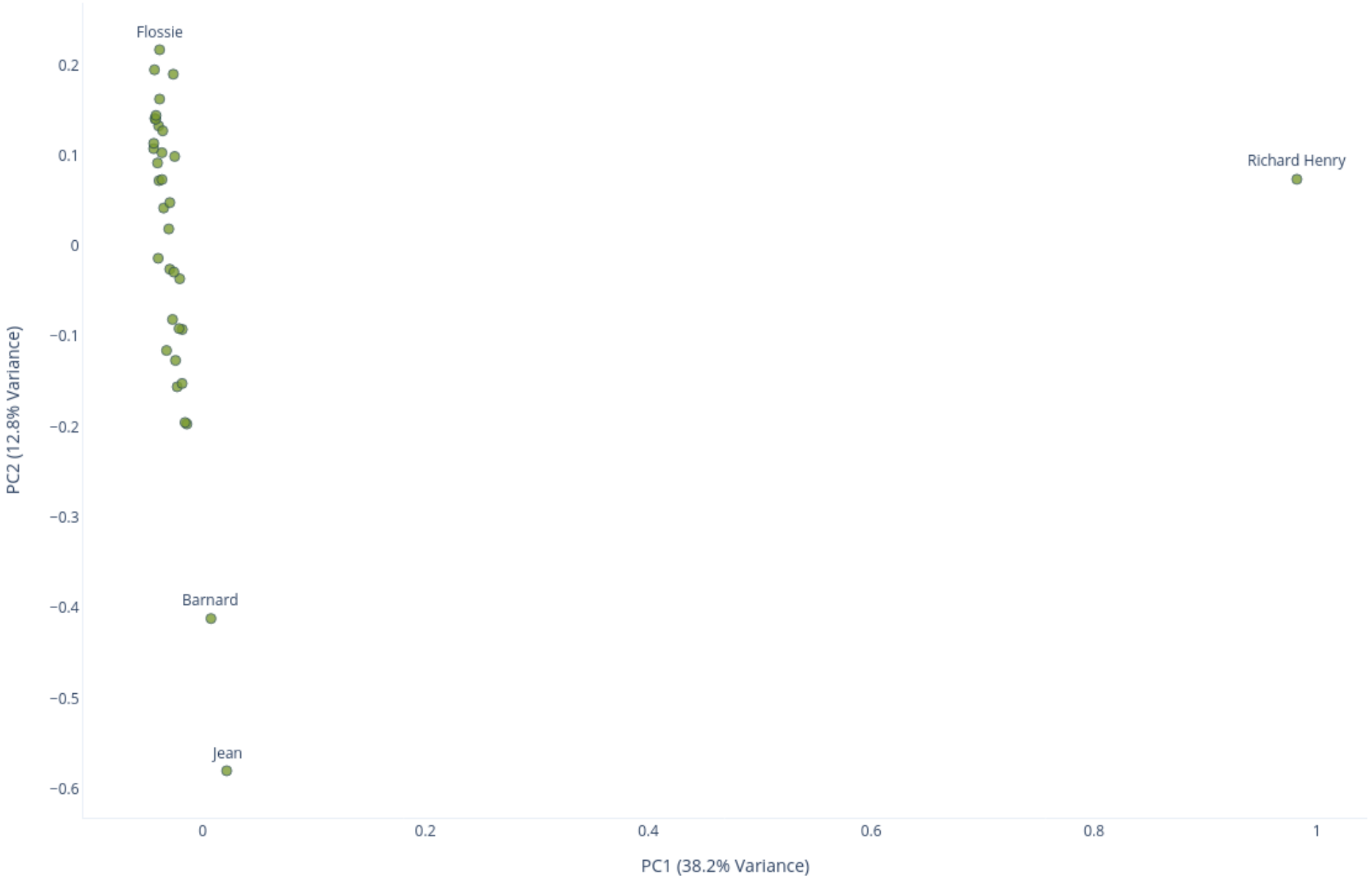
Flossie
Richard Henry
Barnard
Jean
0.2
0.1
0
−0.1
−0.2
−0.3
−0.4
−0.5
−0.6
PC2 (12.8% Variance)
0
0.2
0.4
0.6
0.8
1
PC1 (38.2% Variance)

Supplementary Figure 4. PCA of founders. Founder PCA determined from biallelic SNPs with fewer than 20% missing allele calls and SNP quality >= 99. Half calls set to missing.

Supplementary Figure 5. Local PCA MDS Coordinates 1. Each distinct color represents a different chromosome, starting with S1 (Table S2).

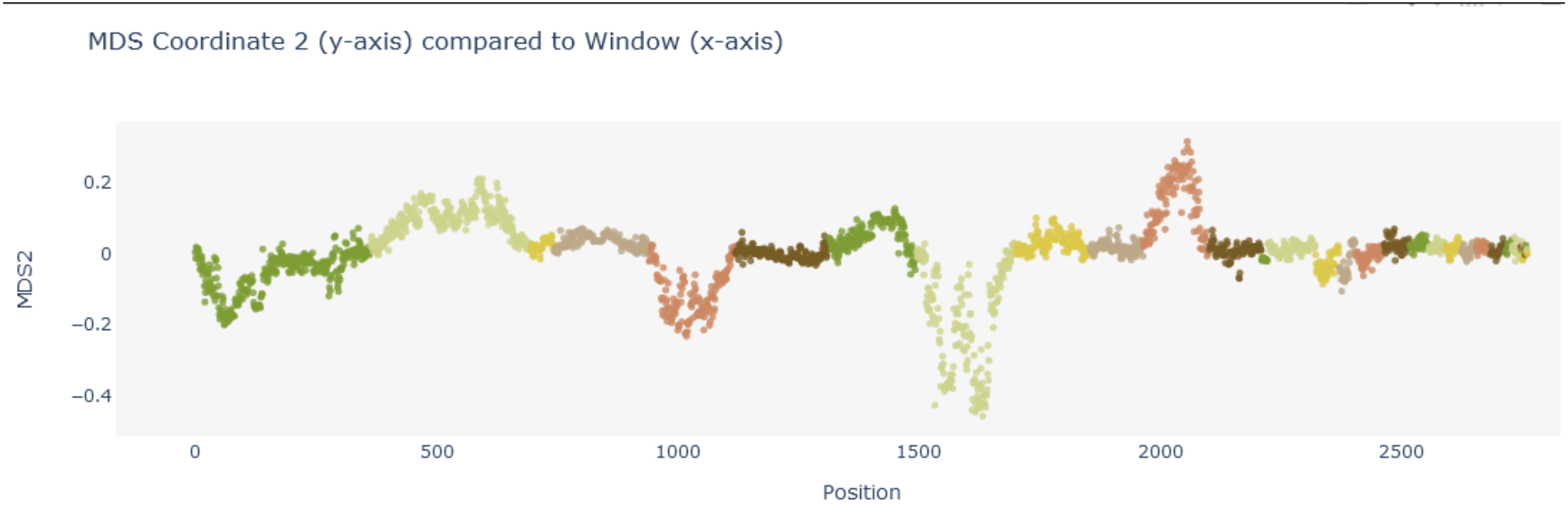

Supplementary Figure 6. Local PCA MDS Coordinates 2. Each distinct color represents a different chromosome, starting with S1 (Table S2)

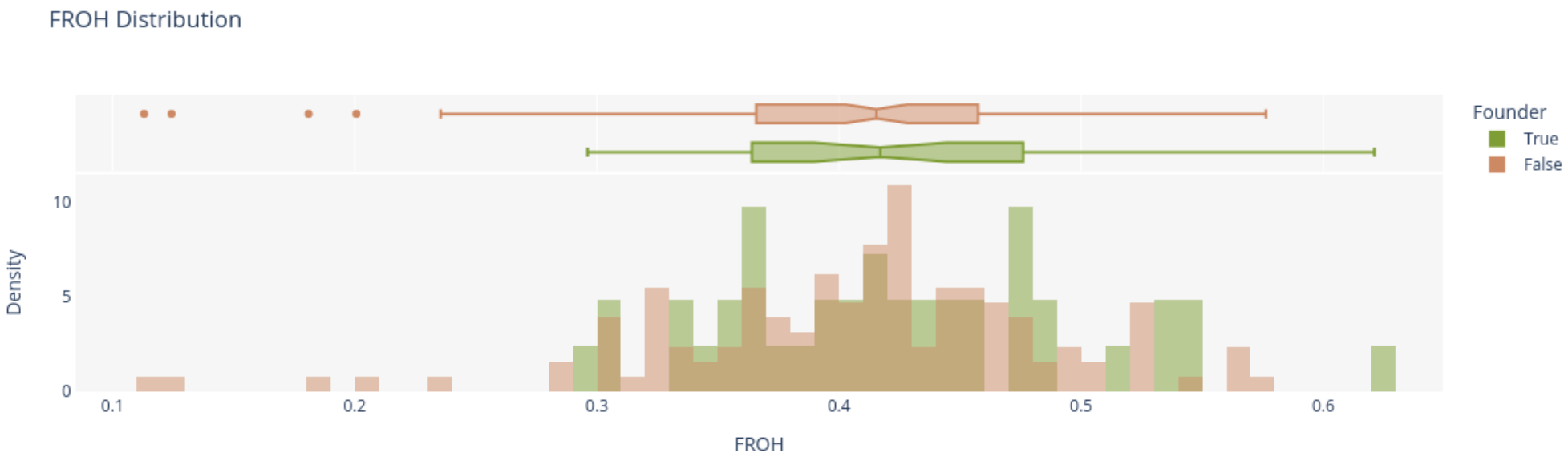

Supplementary Figure 7. Distribution of FROH Length; total portion of the genome covered by runs of homozygosity, per individual. The median error rate is marked as a line inside the box, and the ends of the boxes represent the lower and upper quartiles. Fences are defined as their respective quartile +/- 1.5 times the inter quartile range. Data outside of the fences are plotted individually. n=41 founding members of the population and n=128 non-founders.

Relatedness Evaluation

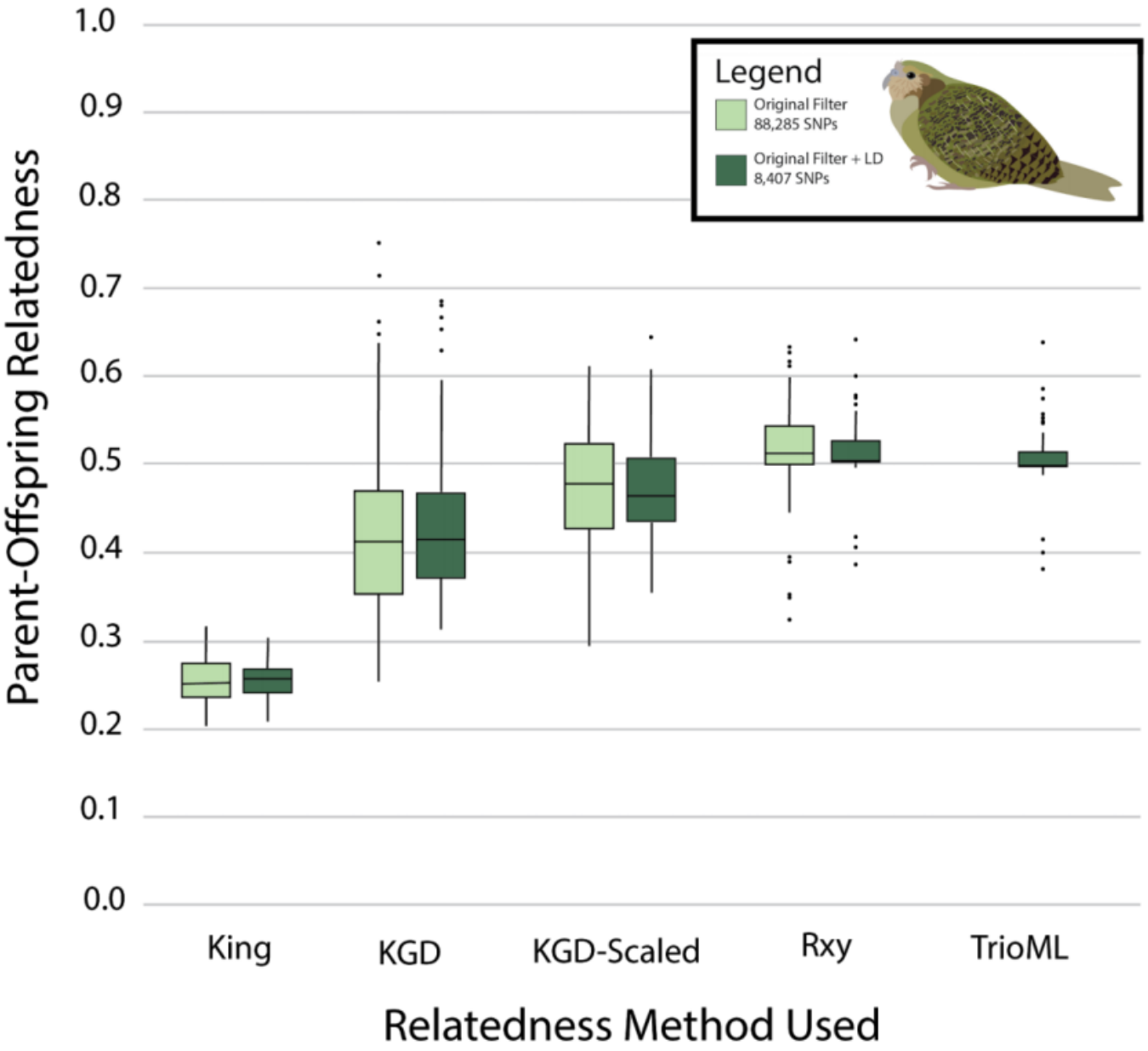

Supplementary Figure 8. Comparison of known parent-offspring relatedness for kākāpō for multiple relatedness estimators.

Multiple relatedness estimators were tested to identify the best method for accurately measuring parent-offspring relatedness to update the studbook and calculate founder-relatedness, including KING (Waples *et al*. 2019, estimated through the package NGSrelateV2, Hanghøj et al. 2019), KGD (Dodds *et al*. 2015), KGD with a correction for self-relatedness (as per Galla *et al*. 2020), R_{xy} (Hendrick & Lacy 2015, estimated through NGSrelateV2), and TrioML (Wang 2007, estimated through the R-programme *related*, Pew et al. 2015). Mother-offspring relationships (n=91) were used to evaluate the precision of relatedness estimators, as first order relationships between parents and offspring should be 0.5 and mother-offspring relationships were confirmed through both field observations and genetic verification. Rxy and TrioML most closely matched our expectation of parent-offspring relatedness of 0.5, with little variance in the estimate, but due to computational costs, Rxy was chosen as the best method for our dataset. Box plot represents the median as the interior line, and boundaries indicate first and third quartiles. Whiskers stretch to 1.5 times the interquartile range, with outlying data plotted individually.

Heritability Simulation

We assessed the accuracy of heritability estimates from Bayesian Alphabet methods and from TASSEL by simulating phenotypes with a range of heritabilities with different numbers of causal SNPs. Simulations were performed on the kākāpō genotypes using simulated phenotypes with R code modified from the hibayes tutorial, as seen in our GitHub repository: https://github.com/GenomicsAotearoa/Kakapo.

These simulations used the default number of iterations and burn-in (20,000 and 14,000, respectively). However, in our phenotypic analysis (Table S2), we set these parameters to 500,000 and 20,000. Simulations consisted of test (one of the available BayesAlphabet functions implemented in hibayes, along with exporting these results and running in Tassel with P3D on and off), simulated heritability ("0.01", "0.05", "0.10", "0.20", "0.30", "0.40", "0.50", "0.60", "0.70", "0.80", "0.90", "0.95", "0.99", "1.0"), and number of SNPs controlling phenotype (10, 100, 1,000, 10,000). For each combination of heritability and number of SNPs, we repeated the simulation 10 times, using a different random number generator for each replicate. The performance of each of the methods was quantified via the error and absolute error of the simulated versus estimated heritability.

Results

After inspection, BayesC and TASSEL's heritability estimates are used in the main text, as they offer the highest accuracy (Fig S4-5) while benefiting from both Bayesian and traditional analysis. In addition, neither appear to suffer extreme error bias at high or low heritabilities (Fig S6). Each test category is the result of n=560 total simulations, as defined above.

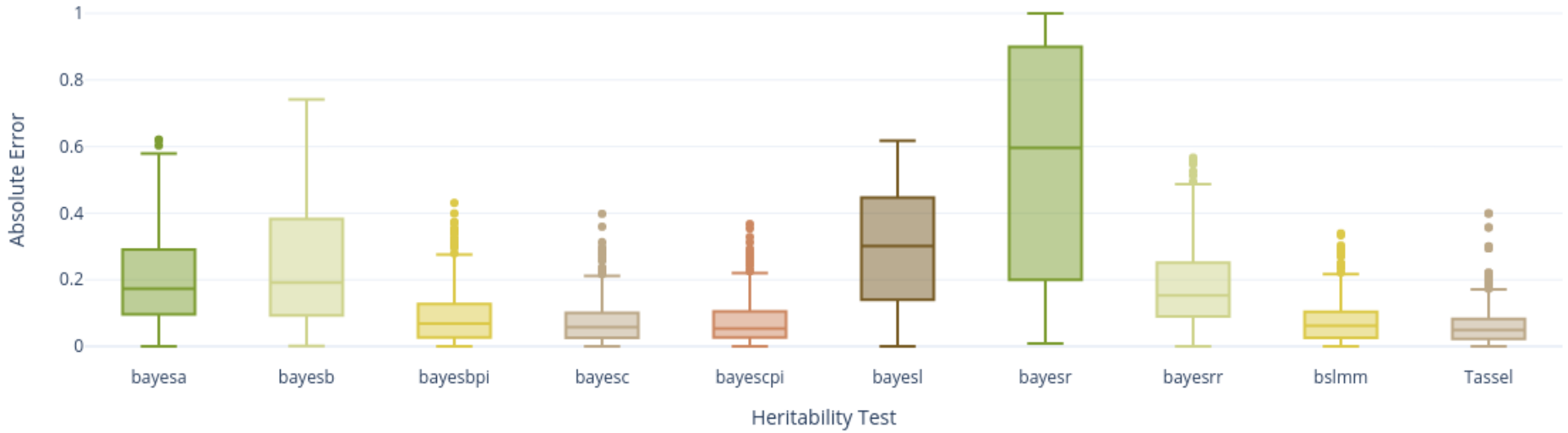

Supplementary Figure 9. Absolute error by test. The median error rate is marked as a line inside the box, and the ends of the boxes represent the lower and upper quartiles. Fences are defined as their respective quartile +/- 1.5 times the inter quartile range. Data outside of the fences are plotted individually.

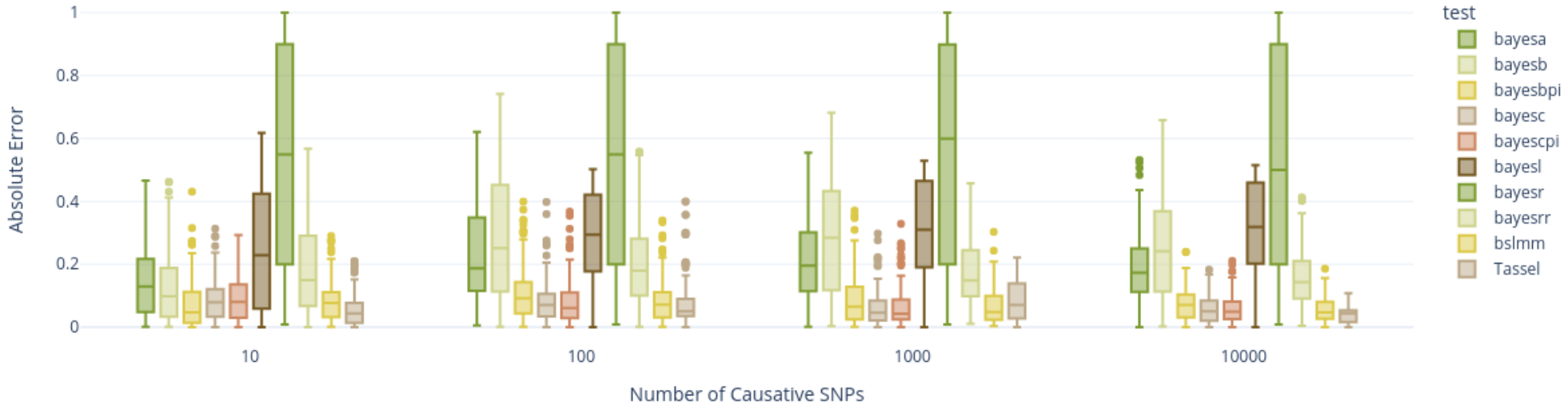

Supplementary Figure 10. Absolute error by number of causative SNPs (k) per test. The median error rate is marked as a line inside the box, and the ends of the boxes represent the lower and upper quartiles. Each box represents n=140 tests. Fences are defined as their respective quartile +/- 1.5 times the inter quartile range. Data outside of the fences are plotted individually.

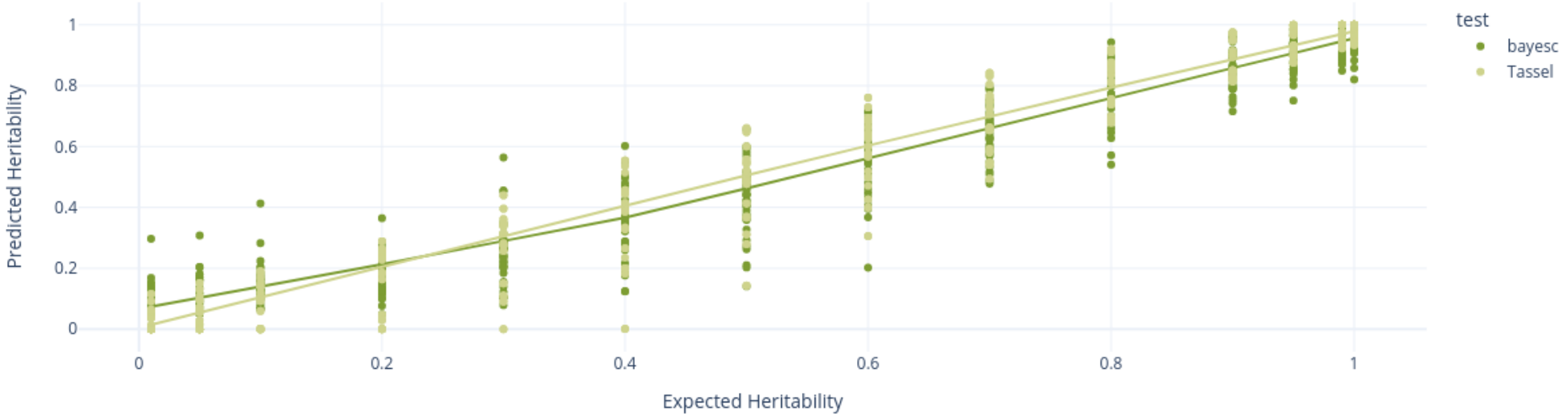

Supplementary Figure 11. Expected vs Predicted heritability for BayesC and TASSEL. A Lowess trendline was fitted for each test.

Breeding Value Calculation Optimization

Simulations were run for 10 replicates, with a 10% chance of a phenotype being masked (unknown phenotypes were not masked). We optimized the parameters for our dataset by testing the following: i) KAML cross-validation number (crv.num), ii) variance components estimation (vc.method), iii) top-SNP correlation threshold (cor.threshold), iv) reference GWAS toggle (ref.gwas), v) GWAS number of principal components used as covariates in the model (gwas.npc). Simulations were measured as the correlation between input values and predicted values of the masked phenotypes. Ideal parameters for our population were: crv.num = 10, vc.method = brent, cor.threshold = 0.90, ref.gwas = FALSE, and gwas.npc = 0.

Phenotype Analyses

Jupyter notebooks are available on our GitHub repository: https://github.com/GenomicsAotearoa/Kakapo
Additional heritability estimates are available in supplemental table S1.

Egg Shape Index

Egg shape index was calculated as width/length, and the mean of these ratios was taken for all measured eggs of each mother. Ratios were 0 centred by subtracting the mean from the ratios. There were a total of 759 observations of egg ratios, with 58 mothers with recorded data. TASSEL predicted a heritability of 0.61, while BayesC estimates heritability was 0.49. Egg Shape Index QQ-plots, manhattan plots, and predicted breeding values are available in Supplementary Figure 8 - 14.

Clutch Size

Clutch size phenotypes were available for 48 individuals in our population dataset with confirmed paternity, spanning the years 1981 - 2021 and included 122 entries, 103 of which were first clutches and 19 were second clutches. We adjusted the raw clutch size phenotypes for each breeding event for contributing factors and for repeated measures across a female's lifetime to give a single adjusted phenotype value for each individual for downstream analyses. To do so, we used TensorFlow probabilistic programming, which enables priors on the mean (termed the 'effect') and standard deviation (termed the 'scale') of the impact of each factor on the phenotype to be updated until the model converges. The model output is a set of distributions of the effects (and standard deviations thereof) for each of the factors on the phenotype. The model was trained with variational inference, which enables variation to be shared across different levels of each effect, which is important in datasets such as this one, where some categories of each factor have very few observations.

In consultation with the Kākapō Recovery Team and by exploring the impact of other possible factors on the raw phenotypes (i.e., via ANOVA - see script: Chick Weights Formatting.ipynb), as well as experimenting with models to find the best fit, the final model fitted was:

Priors

$$
\begin{aligned}
\mu &\sim Uniform(-0.01,\ 0.01) \\
\sigma &\sim Softplus(Uniform(0.01, 1.0)) \\
output\_scale &\sim Softplus(Normal(\mu, \sigma)) \\
rimu\_effect_r &\sim Normal(\mu, \sigma) && \text{for r} = 0, 1 \\
clutch\_effect_c &\sim Normal(\mu, \sigma) && \text{for c} = 0, 1 \\
bird\_effect_b &\sim Normal(\mu, \sigma) && \text{for b} = 0...48 \\
intercept &\sim Normal(2.9016395,\ 0.7289093)
\end{aligned}
$$

The Model

$$
\begin{aligned}
v &\sim intercept + bird\_effect + riperimu\_effect + clutch\_effect \\
y &\sim QuantizedDistribution(Normal(v, output\_scale))
\end{aligned}
$$

Where

$$
\begin{aligned}
r &= \text{rimu unripe (0) or ripe (1)} \\
c &= \text{first (0) or second clutch (1)} \\
b &= \text{mother bird}, 0...48
\end{aligned}
$$

The intercept priors on mean and standard deviation were μ = mean clutch size (2.902) and σ = standard deviation (0.729) of the dataset.
Other prior means are uniformly drawn from random samples between -0.01 and 0.01.

The model was trained as outlined in the Jupyter notebook with loss function defined as the target log probability. The mean loss of the final 1000 steps was 150.319. Convergence was reached when log probability no longer decreased.

A single adjusted phenotype value was taken for each individual as the mean of the individual effect distribution from the model above. This phenotype was then used to estimate trait heritability and for GWAS and breeding value analyses. The heritability of the processed phenotypes was 0.18 from TASSEL and 0.16 from BayesC. Heritabilities estimated with additional methods are listed in Supplemental Table 3.

Predicted model variables are found in Supplementary Figure 15, with the effects of each individual bird in Supplementary Figure 16. Genome-wide association analysis (GWAS) outputs, including QQ Plots and Manhattan plots, are found in Fig S17 - S22. Predicted breeding values are presented in Fig S23.

Growth Rate

Growth rate of chicks was fitted to a Gompertz curve for the first 60 days. Weights were fitted from 8,308 observations, measured from the years 1992 to 2019, for 157 birds, 11 different locations (referred to as islands), and included information on hand-rearing or not. Ripe Rimu was excluded from the dataset as this was captured by Island x Year effects (specified below). Twenty percent of observations, selected randomly, were kept out of the analysis to provide a validation dataset.

We used TensorFlow probabilistic programming to first infer the per-day scale (i.e., standard deviation) across chicks to capture the increasing variance in growth as the chicks get larger over time (in days). To do so, the standard deviation of growth was fitted to a line parameterized by 3 trainable variables (vl[2-4]) and the cumulative distribution function of a logistic distribution parameterized by 2 trainable variables (vl[0], vl[1]). The final formula is as follows:

Variance Day Curve

Priors

$$v_z \sim Uniform(0.0, 2.0) \quad for\ z\ =\ 0 \ldots 4 \tag{2.1}$$

Model

$$\begin{aligned} L &\sim Logistic(v_0,\ |v_1|) \\ f(x) &\sim v_4 * abs(v_3 + v_2 * P(L <= x))] \end{aligned} \tag{2.2}$$

Where

$$\begin{aligned} v_z &= \text{Trainable vector of variables} \\ x &= \text{Age, in days} \\ P(L <= x) &= \text{Cumulative Distribution Function for} \\ &\quad \text{distribution L at point x (day)} \end{aligned}$$

The formula was fitted to reduce the mean absolute percentage error, and trained with the Adam optimizer.

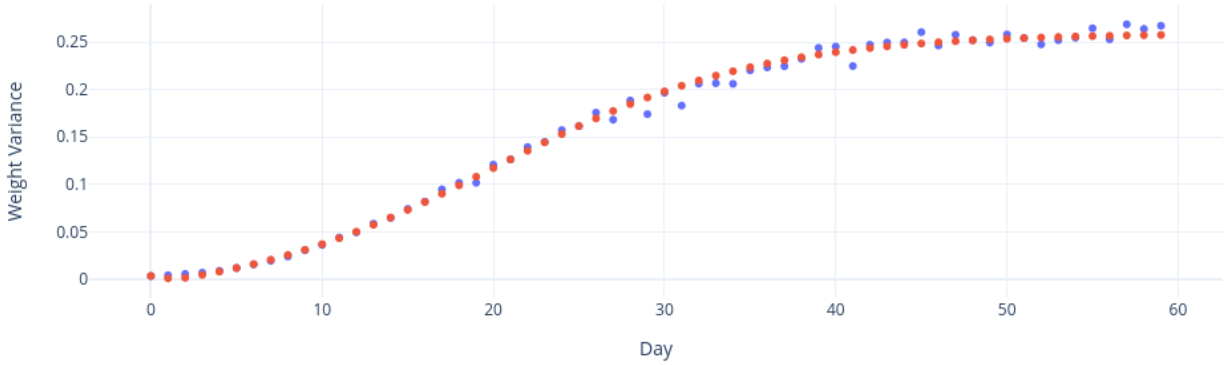

Supplementary Figure 12 The blue dots indicate the actual per-day variance, the red dots is the computed formula.

Once the per-day scale was calculated, the following model was then fit to adjust individual growth for contributing factors across an individual's lifetime to give a single adjusted phenotype value for each individual for downstream analyses. To do so, we used TensorFlow probabilistic programming, which enables priors on the mean (termed the 'effect') and standard deviation (termed the 'scale') of the impact of each factor on the phenotype to be updated until the model converges. The model output is a set of distributions of the effects (and standard deviations thereof) for each of the factors on the phenotype. The model was trained with variational inference, which enables variation to be shared across different levels of each effect, which is important in datasets such as this one, where some categories of each factor have very few observations.

In consultation with the Kākāpō Recovery Team and by exploring the impact of other possible factors on the raw phenotypes (i.e., via ANOVA), as well as experimenting with models to find the best fit, the final model fitted was:

Fit Intercepts

Priors

$$
\begin{aligned}
r &\sim Uniform(0.1, 0.2) \\
\sigma_r &= 1e-8 + Softplus(r) \\
a_{intercept} &\sim Normal(r,\ \sigma_r^2) \\
b_{intercept} &\sim Normal(r,\ \sigma_r^2) \\
M_{intercept} &\sim Normal(r,\ \sigma_r^2)
\end{aligned}
\tag{2.3}
$$

The Model

$$
\begin{aligned}
w &= M \exp(-\exp(a - bx)) \\
y &= Normal(w,\ o)
\end{aligned}
\tag{2.4}
$$

Where

$x =$ Age, in days

$w =$ Weight, as defined by Gompertz

$o =$ Output of (2) with day as input

Fit Effects

Priors

$$\begin{aligned} &\text{for v in } a, b, M: && \text{For each variable in the Gompertz curve} \\ &\quad \text{for } p = 1 \ldots P: && \text{for each random-effect group} \\ &\quad\quad \text{for } c = 1 \ldots |C_p|: && \text{for each category of group } p \\ &\beta_{vpc} \sim Normal(r,\ \sigma_r^2) \end{aligned} \tag{2.5}$$

Model

for i in 1..N : For each data point i

$$\begin{aligned} M_i &= M_{intercept} + \sum_{p=1}^{P} \beta_{M,C_p(i)} \\ a_i &= a_{intercept} + \sum_{p=1}^{P} \beta_{a,C_p(i)} \\ b_i &= b_{intercept} + \sum_{p=1}^{P} \beta_{b,C_p(i)} \\ g(M, a, b, x) &= M \exp(-\exp(a - bx)) \\ y_i | x_i, M_i, a_i, b_i &\sim Normal(g(M_i, a_i, b_i, x_i),\ f(x_i)) \end{aligned} \tag{2.6}$$

Where

$$\begin{aligned} P &= \text{number of random-effect groups} \\ |C_p| &= \text{Number of categories for group } p \\ N &= \text{Number of birds in the dataset} \\ C_p(i) &= \text{Category (under group } p) \text{ of the } i\text{th sample} \\ x &= \text{Age, in days} \\ f(x) &= (2.2) \end{aligned}$$

Random-effect groups included sex (2 levels), year(x), island(x), island by year(x), hand-reared status(2), and ripe rimu status(2)

This part of the model, bird effect for a,b,M are fixed as 0.

Where hr is hand reared status, as provided by the Kākāpō Recovery Team, Year, Island, and Chick are self-explanatory and IslandBy is Island by Year, to capture interaction between the two effects.

The intercept explained ~68% of the data, mean absolute percentage error (MAPE) of 33%. The remaining cofactors (sex, hand-reared status, year, island, island by year) reduced MAPE to ~29% (explaining about 3% of the data). Chicks reduced MAPE to ~6.59% (the dataset left out used for validation was 6.45%). The means are taken for each of the three variables (M, a, b) for each bird to be used as phenotypes in downstream analyses.

Fit Individuals

Priors

for k in 1..157: Number of birds

$$\begin{aligned} M_k &\sim Normal(r, \sigma_r^2) \\ a_k &\sim Normal(r, \sigma_r^2) \\ b_k &\sim Normal(r, \sigma_r^2) \end{aligned} \tag{2.7}$$

Model

for i in 1..N : For each observation i

$$\begin{aligned} M_i &= M_{intercept} + \sum_{p=1}^{P} \beta_{M,C_p(i)} + M_k(\\ a_i &= a_{intercept} + \sum_{p=1}^{P} \beta_{a,C_p(i)} + a_k(i) \\ b_i &= b_{intercept} + \sum_{p=1}^{P} \beta_{b,C_p(i)} + b_k(i) \\ g(M_i, a_i, b_i, x_i) &= M_i \exp(-\exp(a_i - b_i x)) \\ y_i | x_i, M_i, a_i, b_i &\sim Normal(g(M_i, a_i, b_i, x_i),\ f(x_i)) \end{aligned} \tag{2.8}$$

Where

N = Each observation of age (days), sex, year, island, weight, island by year, ha
There are a total of 8,308 observations used

p_i = Bird for individual i

Growth rate GWAS results and predicted breeding values are found in Figures S24-44.

Fertile Eggs

Fertile egg phenotype data, as determined by the conservation management team, consisted of 122 observations from 48 mothers and 37 confirmed fathers, across 6 islands, across 15 years (ranging from 1981 - 2021) and was calculated as the ratio of reported fertile eggs to the total clutch size. Each mother had between 1 and 6 observations (mean; μ = 2.54, standard deviation; σ = 1.54). Fathers had between 1 and 14 observations (μ = 3.30, σ = 2.88). Mating pairs were unique in 91 observations, and 12 pairs had repeated pairings, with between 2 and 6 pairing events (μ = 2.58, σ = 1.24). The fertile egg ratio across all observations had μ = 0.89 and σ =0.22.

We adjusted the fertile egg ratio for each breeding event for contributing factors to give a single adjusted phenotype value for each female for downstream analyses. To do so, we used TensorFlow probabilistic programming, which enables priors on the mean (termed the 'effect') and standard deviation (termed the 'scale') of the impact of each factor on the phenotype to be updated until the model converges. The model output is a set of distributions of the effects (and standard deviations thereof) for each of the factors on the phenotype.

In consultation with the Kākāpō Recovery Team and by exploring the impact of other possible factors on the raw phenotypes (i.e., via ANOVA), as well as experimenting with models to find the best fit, the final joint distribution model fitted was as follows:

Priors

$$
\begin{aligned}
\mu &\sim Uniform(0.0,\ 3.0) \\
\sigma &\sim 1e-8 + Softplus(Uniform(0.01, 1.0)) \\
bird\_effect &\sim Normal(\mu,\ \sigma) && \text{For } 1...48 \\
father\_effect &\sim Normal(\mu,\ \sigma)) && \text{For } 1...37 \\
output\_scale &\sim Normal(\mu,\ \sigma) \\
intercept &\sim Normal(\mu,\ \sigma)
\end{aligned}
$$

The Model

$$
\begin{aligned}
loc &= intercept + bird\_effect * father\_effect \\
scale &= sigmoid(output\_scale) \\
y &\sim Normal(loc, scale)
\end{aligned}
$$

Where

$$
\begin{aligned}
\text{sigmoid}(x) &= 1/(1+\exp(-x)) \\
\text{softplus}(x) &= log(exp(x)+1)
\end{aligned}
$$

Scale is the sigmoid of the smallest value of bird_scale or father_scale, added with 1e-4, to prevent the scale from reaching zero. This was determined from multiple experiments to identify a working model. The loss function is the target log probability. The final loss is ~53. Model results and GWAS Results are found in Figs S45-53.

Embryo Survival

Embryo survival phenotype is from the same dataset as Fertile Eggs. Embryo survival is defined as (1 - (dead embryo count / fertile eggs)) per clutch, and the ratio across all observations had μ = 0.81 and σ =0.28.

Priors

$$
\begin{aligned}
\mu &\sim Uniform(-0.01,\ 0.01) \\
\sigma &\sim Uniform(0.5, 1.0) \\
bird\_effect &\sim Normal(\mu,\ \sigma) && \text{For } 1...48 \\
zfather\_effect &\sim Normal(\mu,\ \sigma)) && \text{For } 1...37 \\
bird\_scale &\sim Softplus(Normal(\mu,\ \sigma)) && \text{For } 1...48 \\
father\_scale &\sim Softplus(Normal(\mu,\ \sigma)) && \text{For } 1...37 \\
intercept &\sim Normal(\mu,\ \sigma)
\end{aligned}
$$

The Model

$$
\begin{aligned}
loc &= intercept + bird\_effect * father\_effect \\
scale &= sigmoid(minimum(bird\_scale, father\_scale)) \\
y &\sim Normal(loc, scale) \\
\mathbf{sigmoid}(x) &= 1/(1 + \exp(-x)) \\
\mathbf{softplus}(x) &= log(exp(x) + 1)
\end{aligned}
$$

We adjusted the embryo survival ratio for each breeding event for contributing factors to give a single adjusted phenotype value for each female for downstream analyses. To do so, we used variational inference TensorFlow probabilistic programming, which enables priors on the mean (termed the ‘effect’) and standard deviation (termed the ‘scale’) of the impact of each factor on the phenotype to be updated until the model converges. The model output is a set of distributions of the effects (and standard deviations thereof) for each of the factors on the phenotype.

In consultation with the Kākāpō Recovery Team and by exploring the impact of other possible factors on the raw phenotypes (i.e., via ANOVA), as well as experimenting with models to find the best fit, the final joint distribution model fitted was as follows:

Model training was performed as Fertile Eggs, and the average loss of the final 1000 steps was 154.87. GWAS Results are found in Figures S54 - S60.

Aspergillosis Susceptibility

The 2019 Aspergillosis outbreak–restricted to a single island (Whenua Hou)–was of urgent concern, with 25 infections and 10 deaths at the time of the dataset analysis. As many of the infected chicks did not have sequence information available, parents were used as a proxy for these individuals. For each infected individual with genetic data (n = 4), we defined aspergillosis susceptibility as 1. In the absence of genotype information for an infected individual (n = 21), we assigned its two genotyped parents an aspergillosis susceptibility, defined as the ratio of the total number of their infected offspring to the total clutch size. Aspergillosis offspring ratios ranged from 0.08 to 0.75 for uninfected parents. Given that many individuals were not exposed to aspergillosis, uninfected individuals were assigned a missing phenotype value (rather than defined with susceptibility = 0) for the GWAS and breeding value calculations. Model and GWAS Results are found in Figures S61 - S68.

Phenotype Results

Egg Shape Index

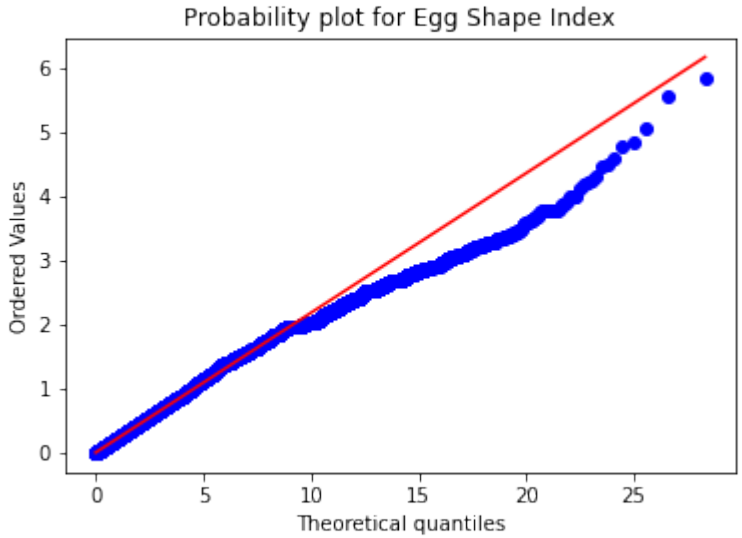

Supplementary Figure 13. QQ-Plot for Egg Shape Index marker p-values from Mixed Linear Model GWAS test.

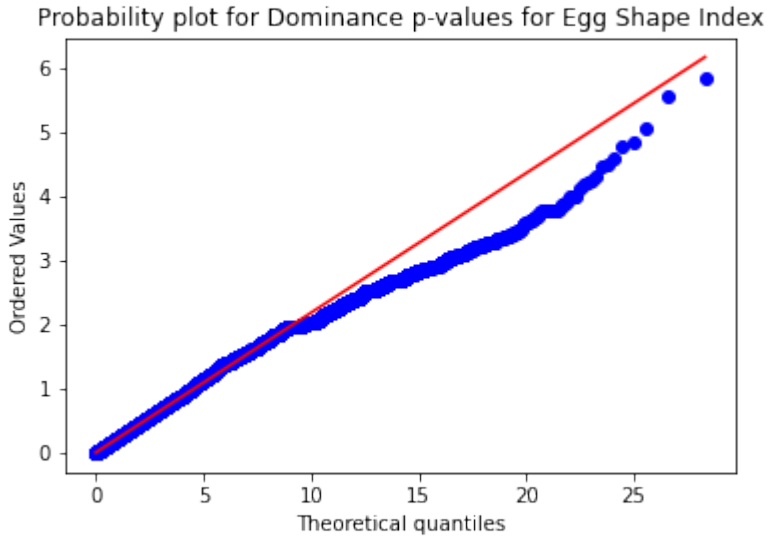

Supplementary Figure 14. QQ-Plot for Egg Shape Index marker p-values, Dominance model, from Mixed Linear Model GWAS test.

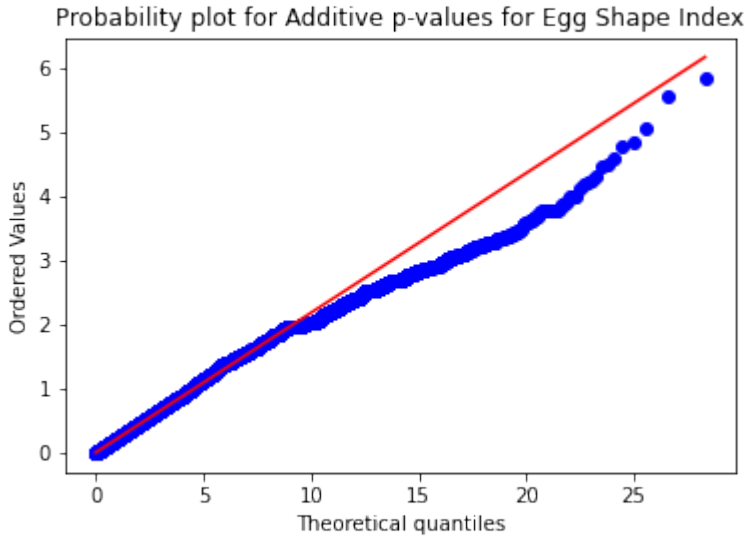

Supplementary Figure 15. QQ-Plot for Egg Shape Index marker p-values, Additive model, from Mixed Linear Model GWAS test.

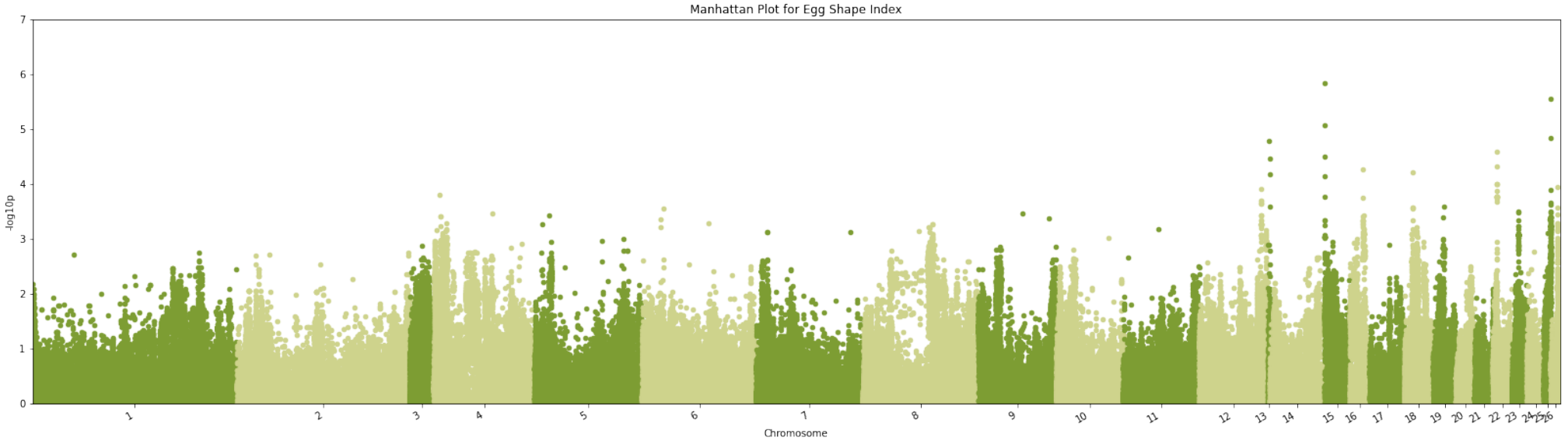

Supplementary Figure 16. Manhattan plot of -log10(p) using the marker p-value from TASSEL GWAS Mixed Linear Model for Egg Shape Index for chromosomes 1 through 26 (Supplemental Table S2 for Chromosome mapping).

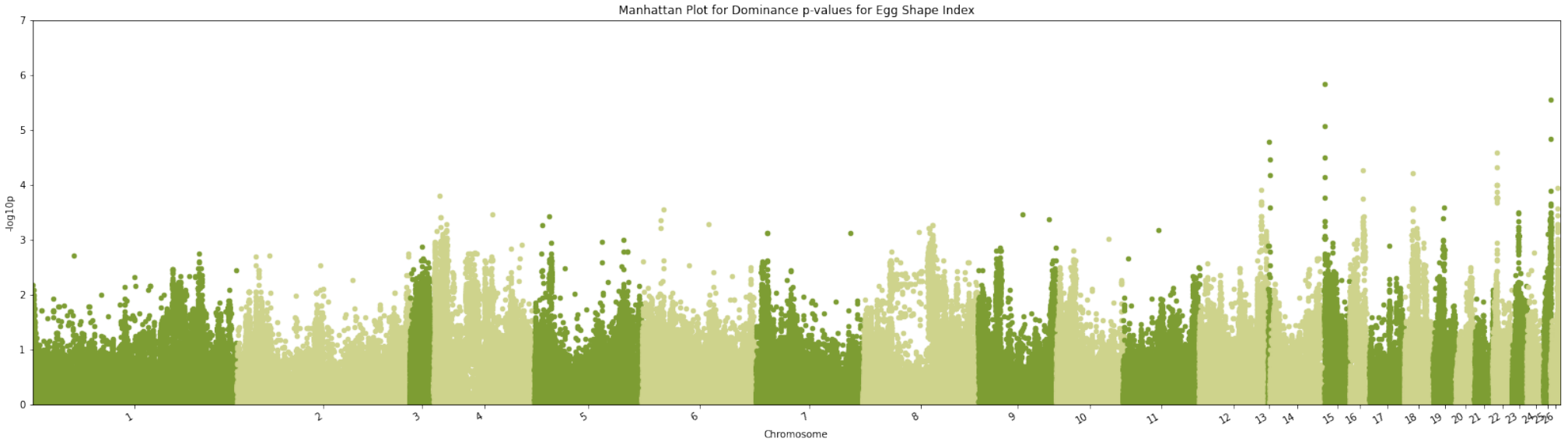

Supplementary Figure 17. Manhattan plot -log10(p) using the marker p-value from TASSEL GWAS Mixed Linear Model for Egg Shape Index for chromosomes 1 through 26 (Supplemental Table S2 for Chromosome mapping), Dominance model.

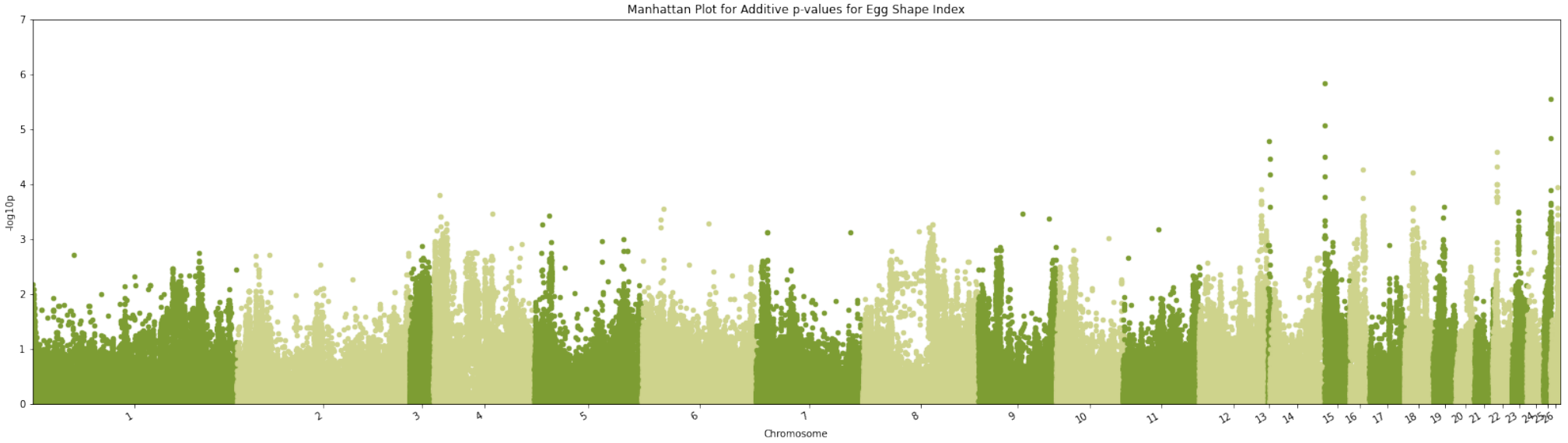

Supplementary Figure 18. Manhattan plot -log10(p) using the marker p-value from TASSEL GWAS Mixed Linear Model for Egg Shape Index for chromosomes 1 through 26 (Supplemental Table S2 for Chromosome mapping), Additive.

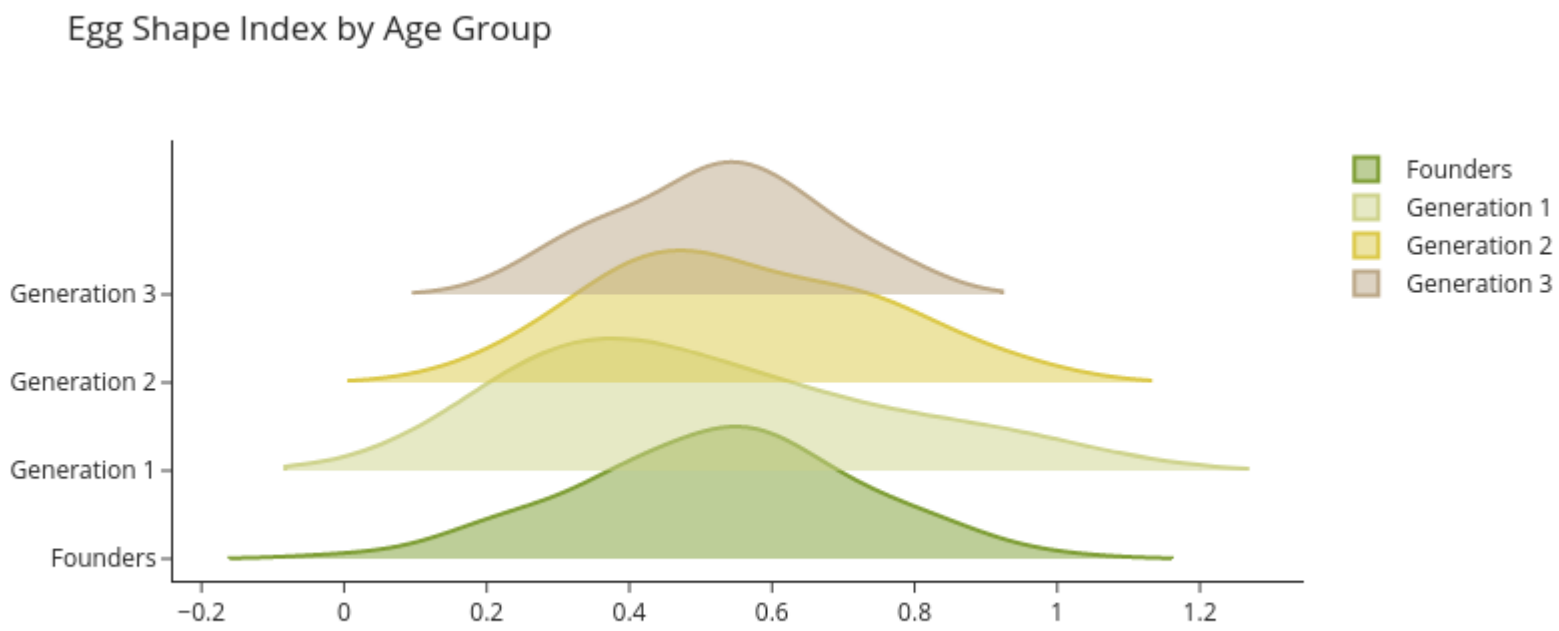

Supplementary Figure 19. Predicted breeding values by age group (Table 1) for Egg Shape Index.

Supplementary Figure 20. Clutch size effect estimates for the model. Boxes are derived from sampling the underlying posterior distributions n=10,000 times and plotting the results. The median effect size is marked as a line inside the box, and the ends of the boxes represent the lower and upper quartiles. Fences are defined as their respective quartile +/- 1.5 times the inter quartile range. Data outside of the fences are plotted individually.

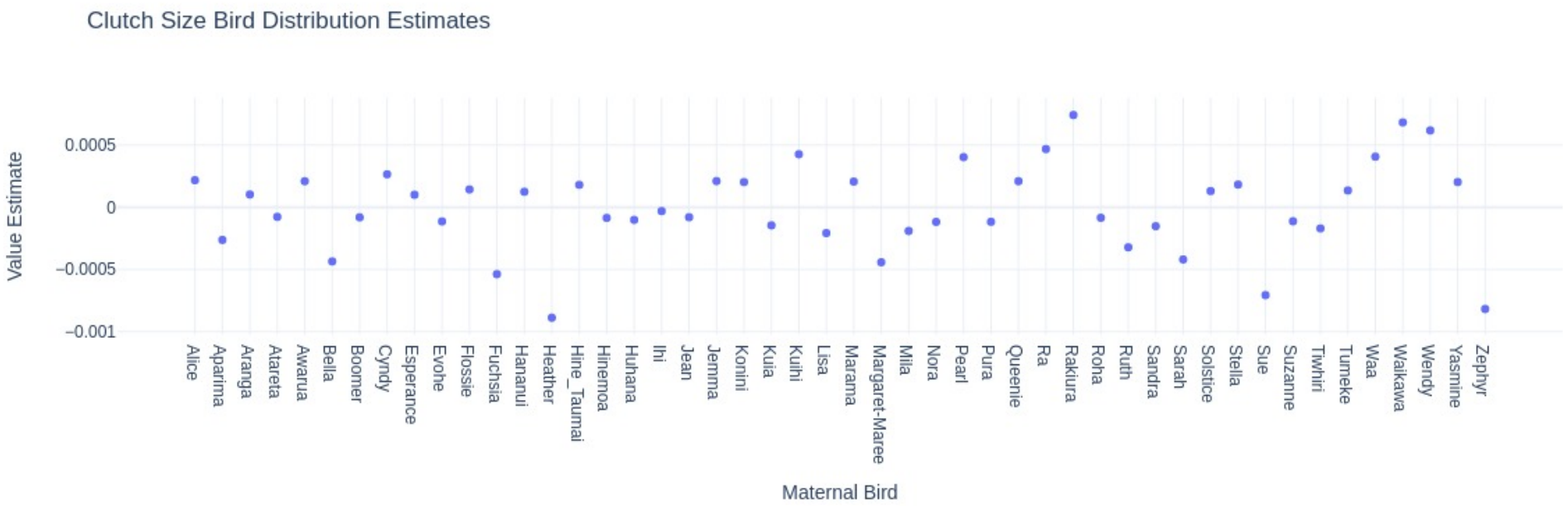

Supplementary Figure 21. Clutch size effect estimate for mother birds.

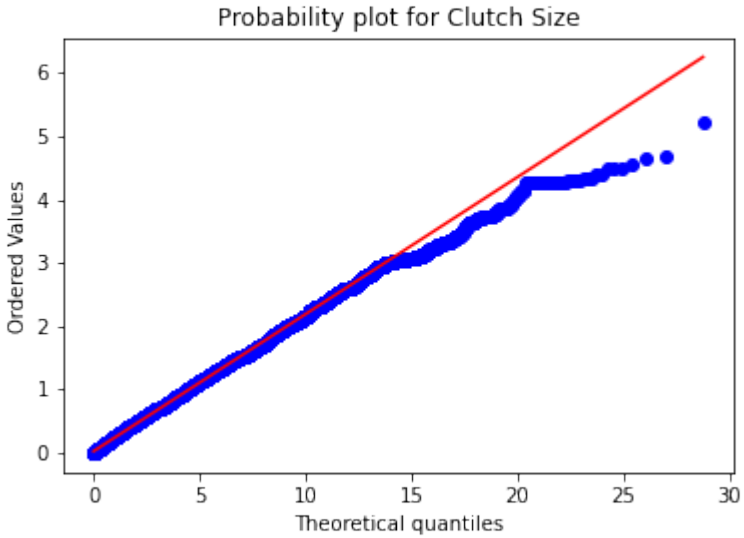

Supplementary Figure 22. Clutch size QQ-plot for marker p-values, from Mixed Linear Model GWAS test.

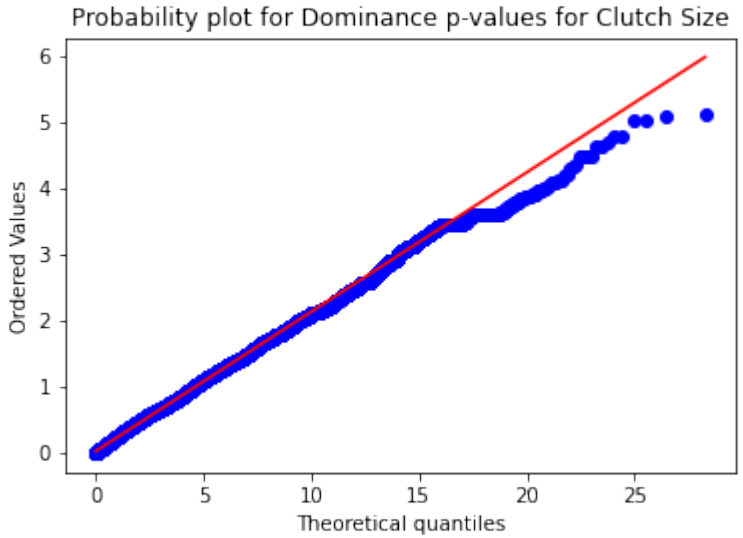

Supplementary Figure 23. Clutch size QQ-plot for dominance p-values, from Mixed Linear Model GWAS test.

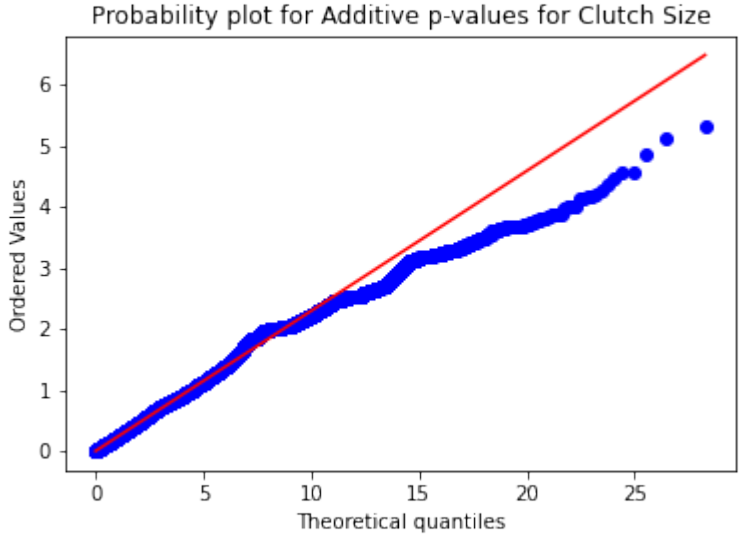

Supplementary Figure 24. Clutch size QQ-plot for additive p-values, from Mixed Linear Model GWAS test.

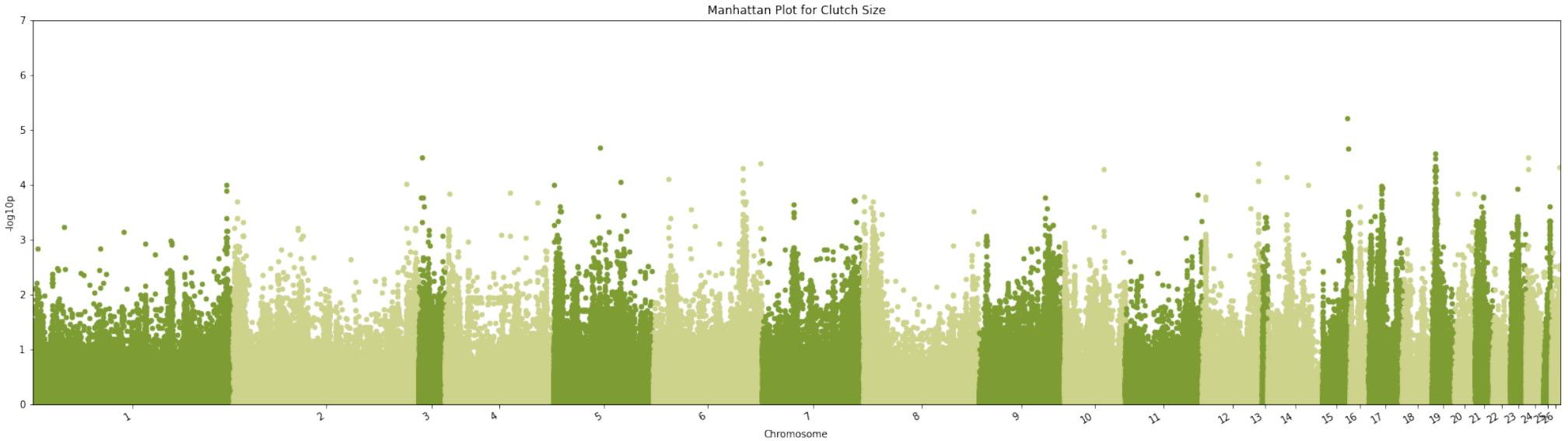

Supplementary Figure 25. Manhattan plot -log10(p) using the marker p-value from TASSEL GWAS Mixed Linear Model for Clutch Size for chromosomes 1 through 26 (Supplemental Table S2 for Chromosome mapping).

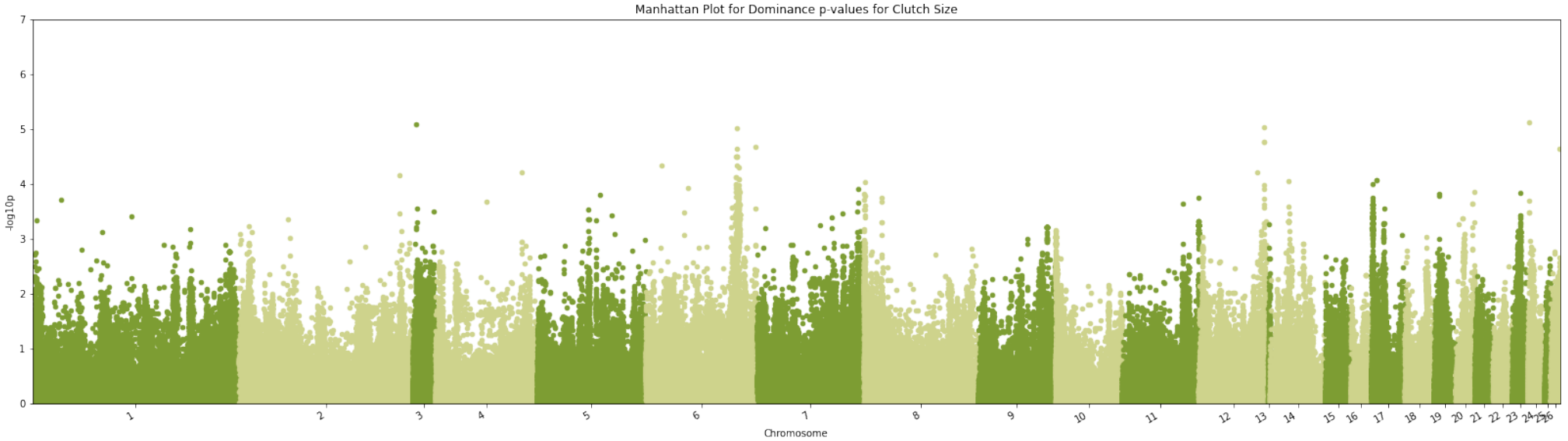

Supplementary Figure 26. Manhattan plot -log10(p) using the marker p-value from TASSEL GWAS Mixed Linear Model for Clutch Size for chromosomes 1 through 26 (Supplemental Table S2 for Chromosome mapping). Dominance model.

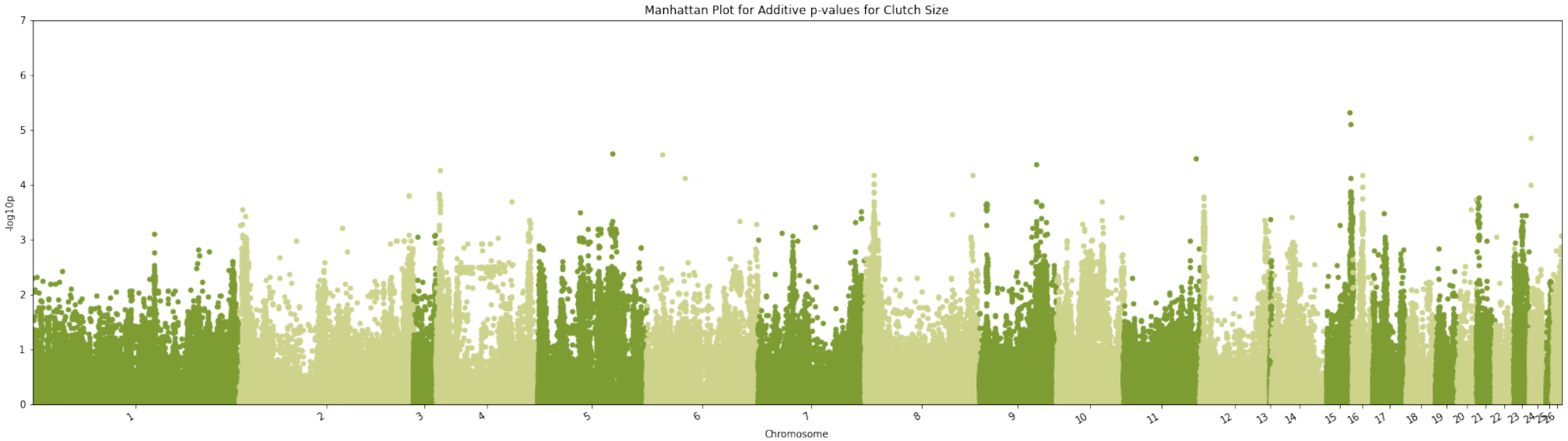

Supplementary Figure 27. Manhattan plot -log10(p) using the marker p-value from TASSEL GWAS Mixed Linear Model for Clutch Size for chromosomes 1 through 26 (Supplemental Table S2 for Chromosome mapping). Additive model.

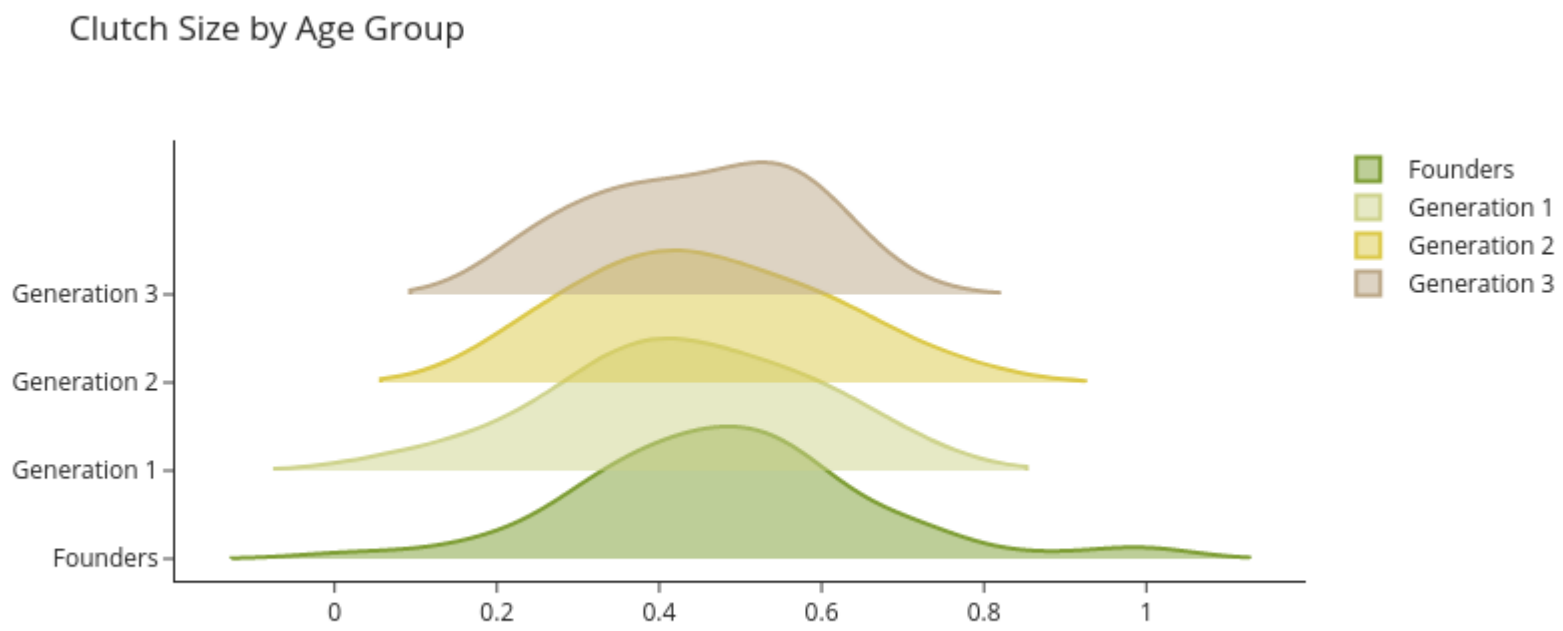

Supplementary Figure 28. Predicted breeding values by age group for Clutch Size.

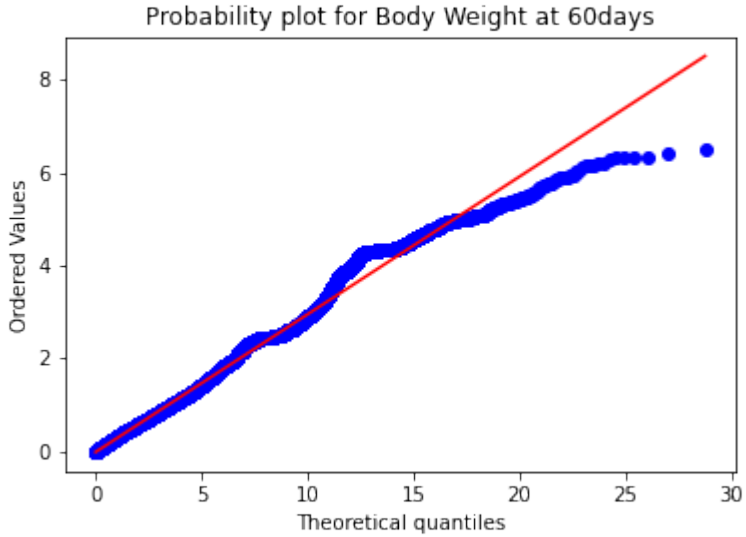

Supplementary Figure 29. Body Weight at 60days QQ-plot, from Mixed Linear Model GWAS test.

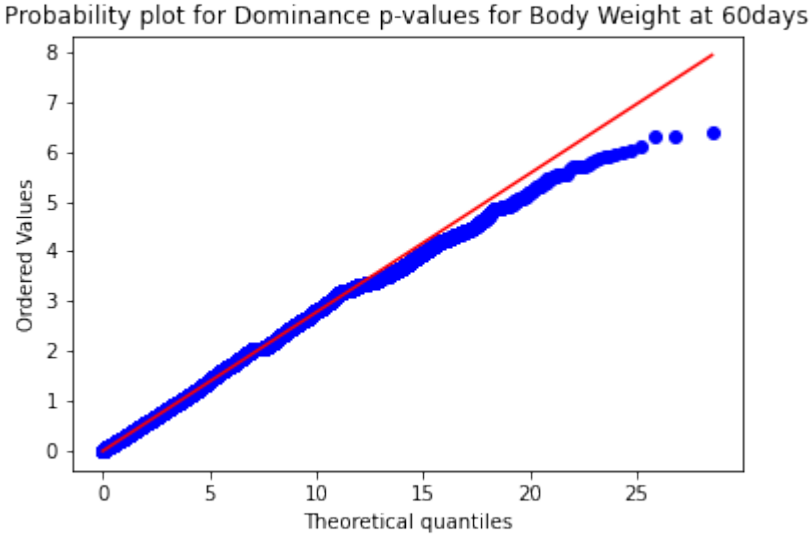

Supplementary Figure 30. Body Weight at 60days QQ-plot. Dominance model, from Mixed Linear Model GWAS test.

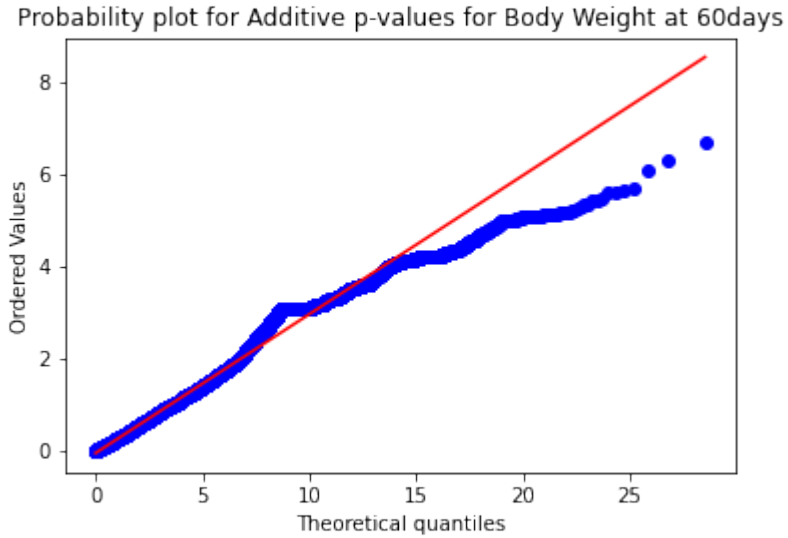

Supplementary Figure 31. Body Weight at 60days QQ-plot. Dominance model, from Mixed Linear Model GWAS test.

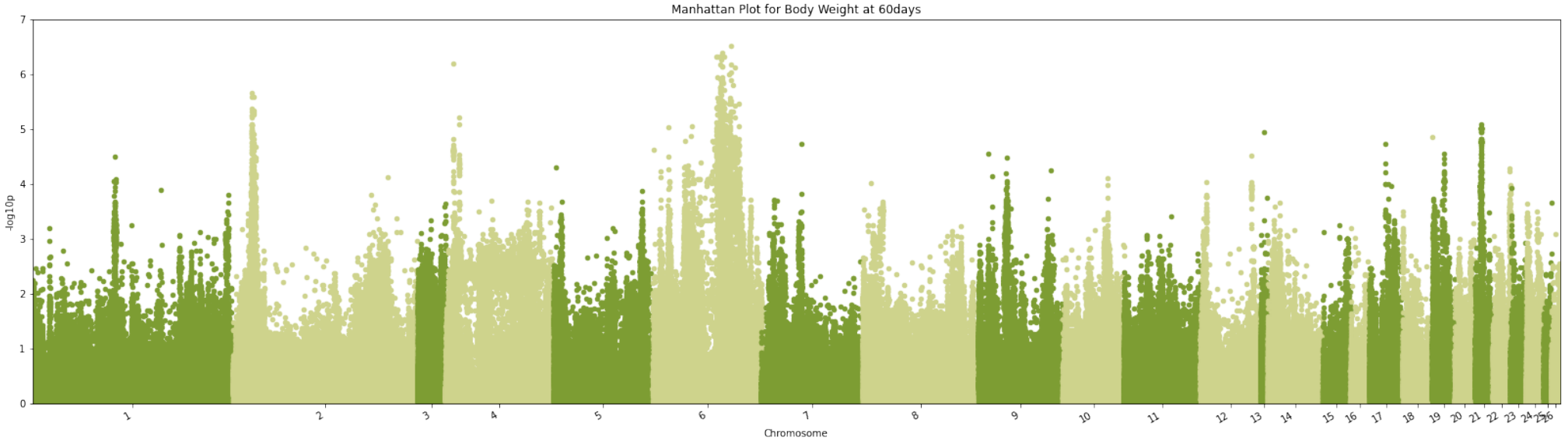

Supplementary Figure 32. Manhattan plot -log10(p) using the marker p-value from TASSEL GWAS Mixed Linear Model for Body Weight at 60 days for chromosomes 1 through 26 (Supplemental Table S2 for Chromosome mapping).

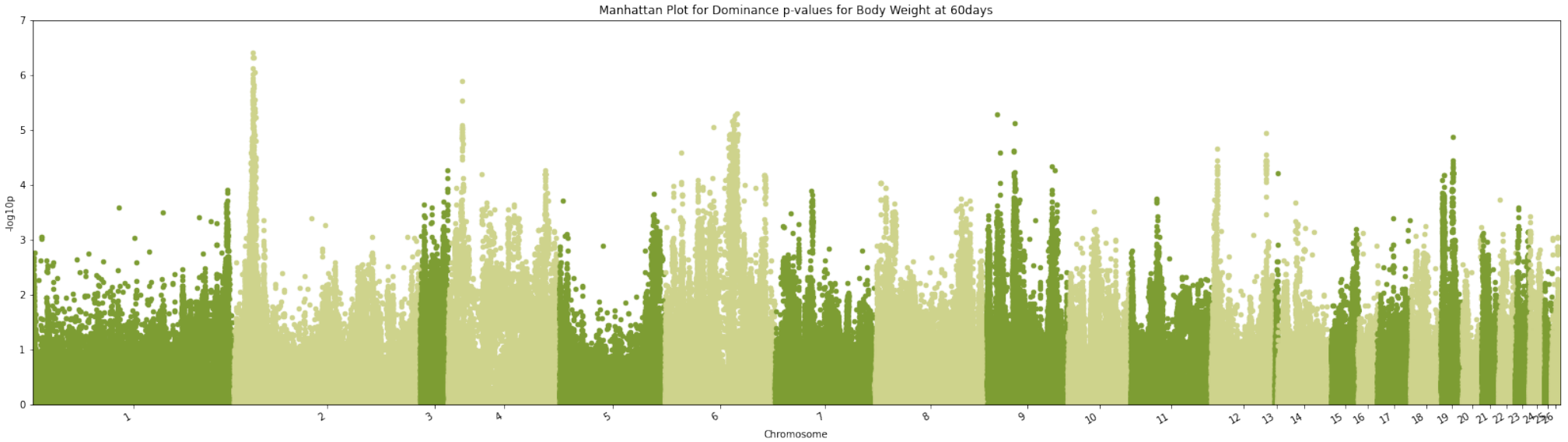

Supplementary Figure 33. Manhattan plot -log10(p) using the marker p-value from TASSEL GWAS Mixed Linear Model for Body Weight at 60 days for chromosomes 1 through 26 (Supplemental Table S2 for Chromosome mapping). Dominance model.

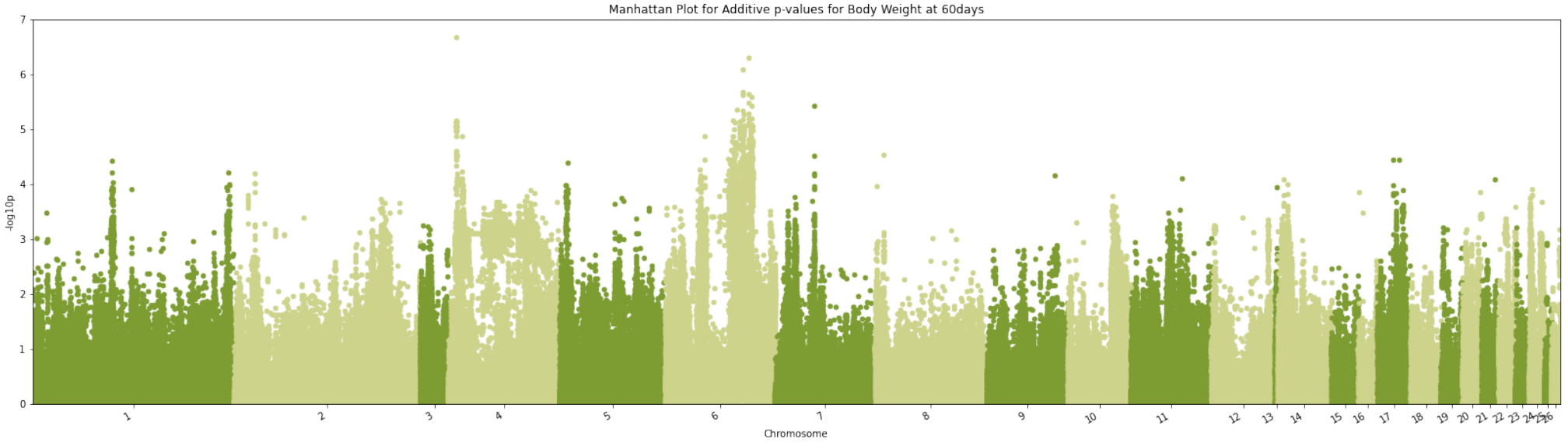

Supplementary Figure 34. Manhattan plot -log10(p) using the marker p-value from TASSEL GWAS Mixed Linear Model for Body Weight at 60 days for chromosomes 1 through 26 (Supplemental Table S2 for Chromosome mapping). Additive model.

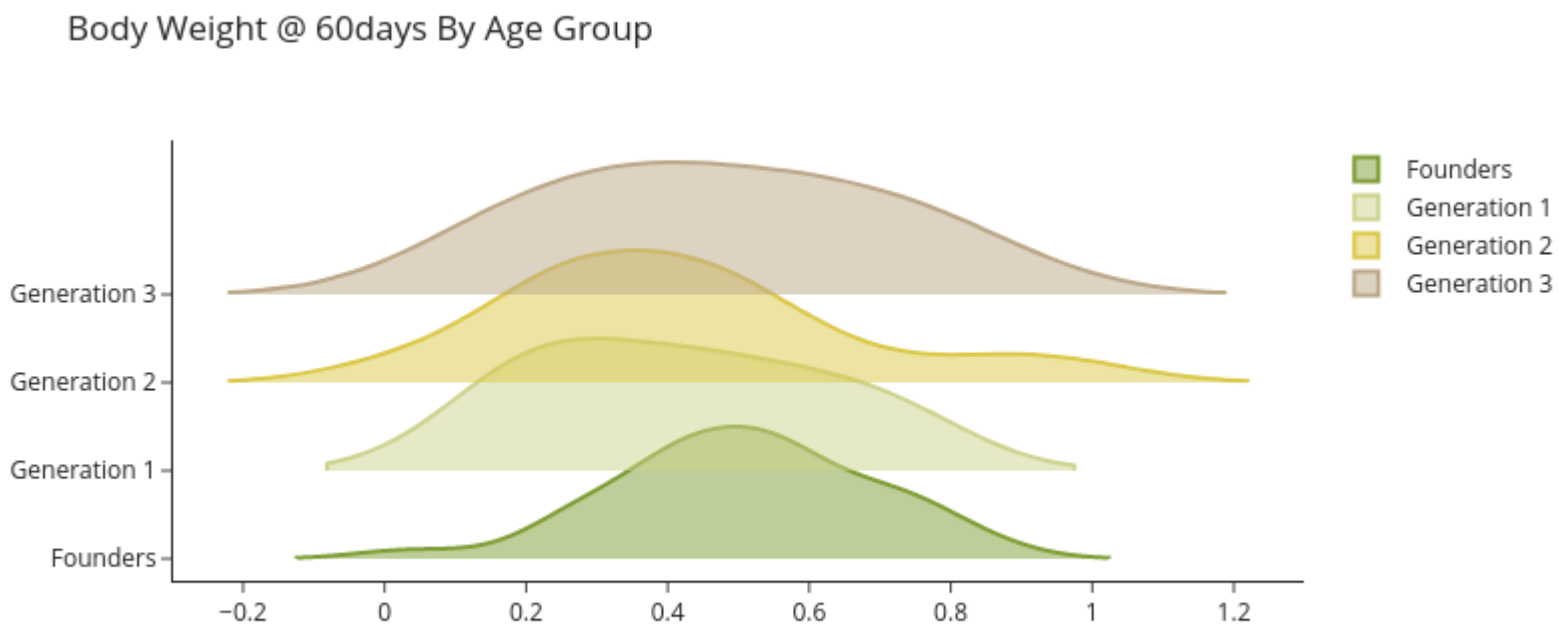

Supplementary Figure 35. Predicted breeding values by age group for Body Weight at 60 days.

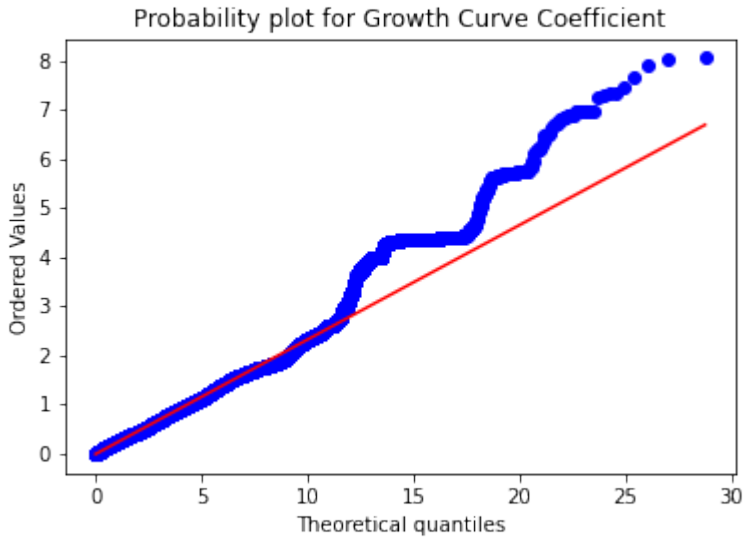

Supplementary Figure 36. Growth Curve Coefficient (Gompertz Curve) QQ-Plot, from Mixed Linear Model GWAS test.

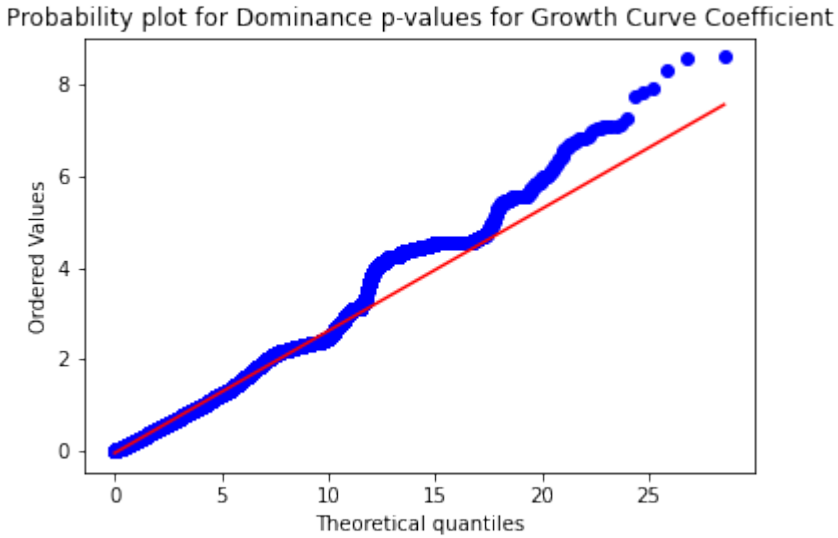

Supplementary Figure 37. Growth Curve Coefficient (Gompertz Curve) QQ-Plot. Dominance model, from Mixed Linear Model GWAS test.

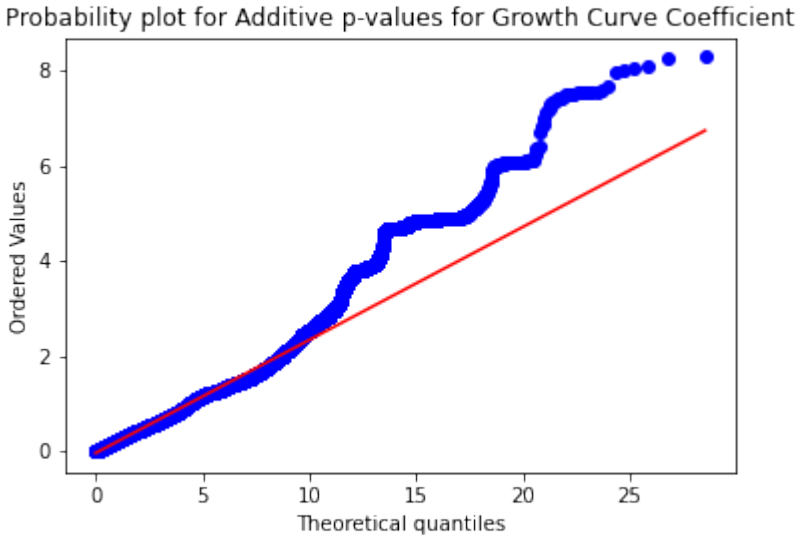

Supplementary Figure 38. Growth Curve Coefficient (Gompertz Curve) QQ-Plot. Additive model, from Mixed Linear Model GWAS test.

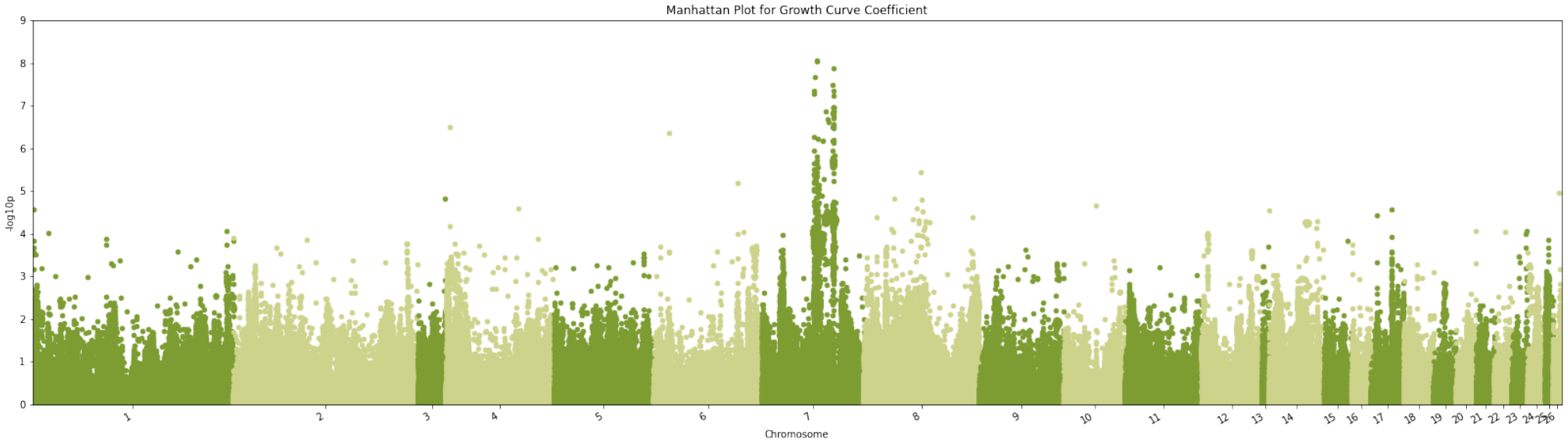

Supplementary Figure 39. Manhattan plot -log10(p) using the marker p-value from TASSEL GWAS Mixed Linear Model for Growth Curve Coefficient for chromosomes 1 through 26 (Supplemental Table S2 for Chromosome mapping).

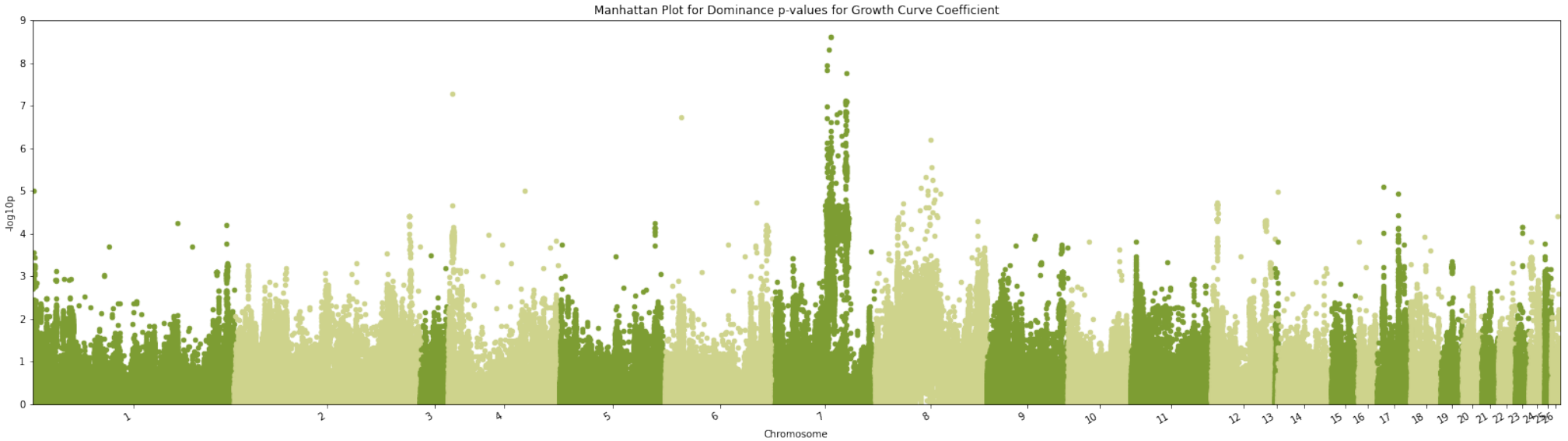

Supplementary Figure 40. Manhattan plot -log10(p) using the marker p-value from TASSEL GWAS Mixed Linear Model for Growth Curve Coefficient for chromosomes 1 through 26 (Supplemental Table S2 for Chromosome mapping). Dominance model.

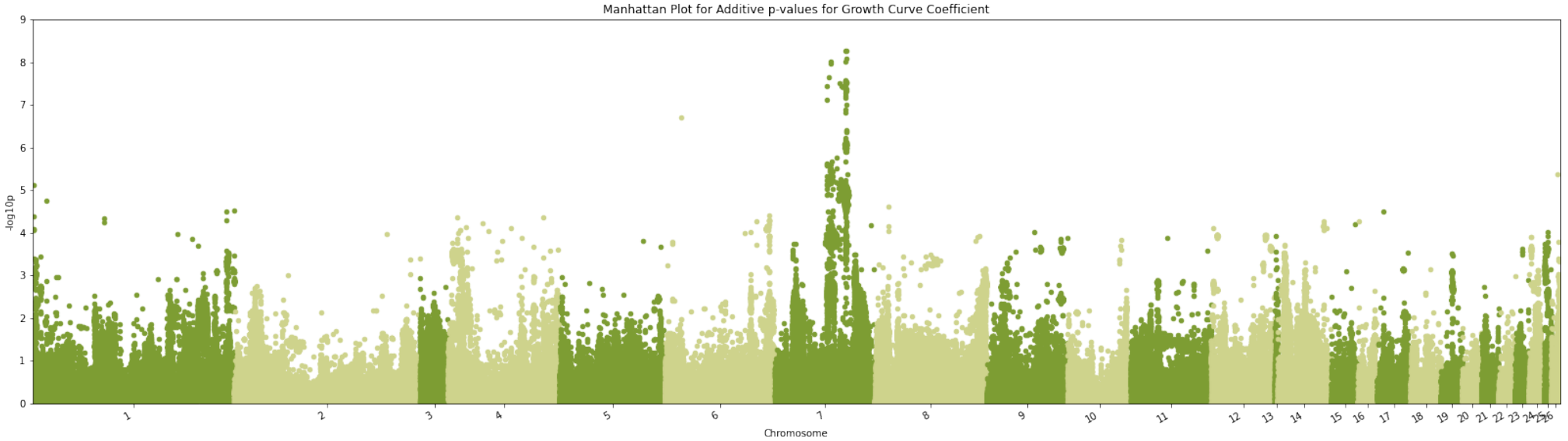

Supplementary Figure 41. Manhattan plot -log10(p) using the marker p-value from TASSEL GWAS Mixed Linear Model for Growth Curve Coefficient for chromosomes 1 through 26 (Supplemental Table S2 for Chromosome mapping). Additive model.

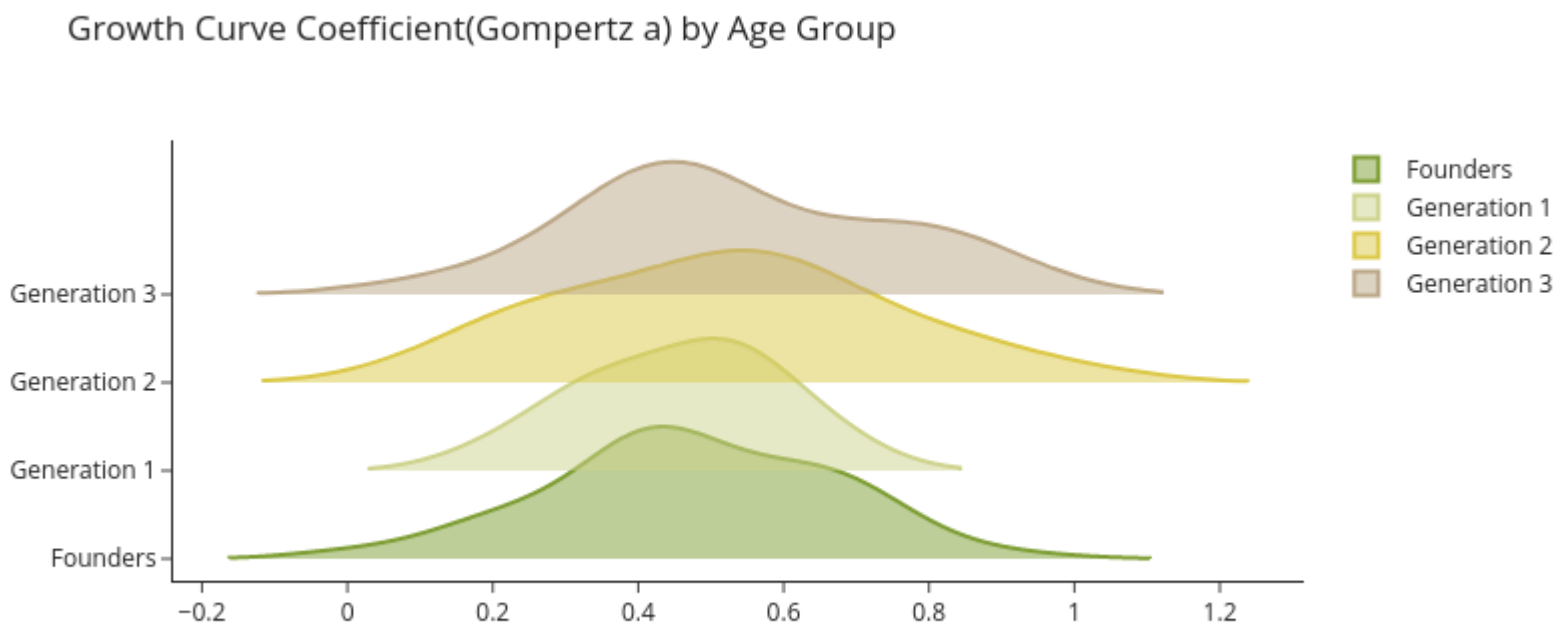

Supplementary Figure 42. Predicted breeding values by age-group for Gompertz Growth Curve Coefficient.

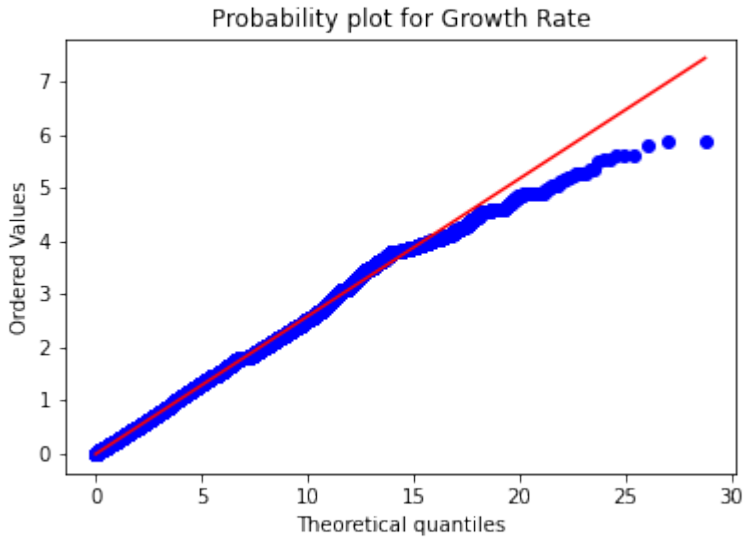

Supplementary Figure 43. Growth Curve Growth Rate (Gompertz Curve) QQ-Plot, from Mixed Linear Model GWAS test.

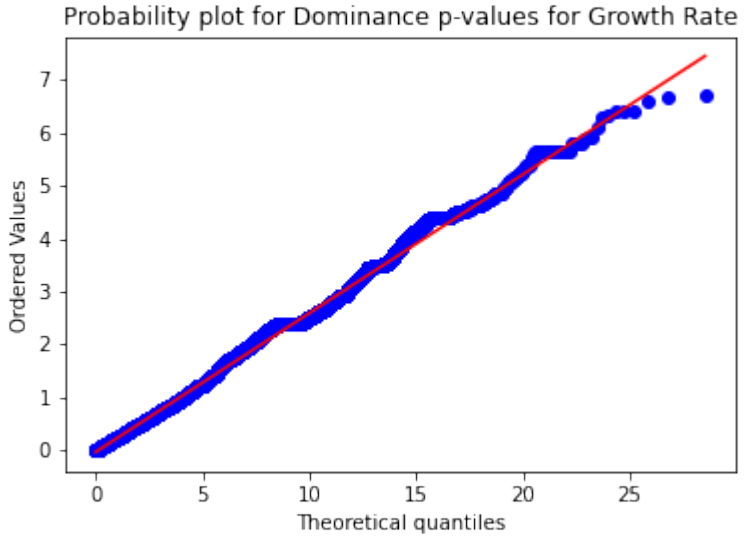

Supplementary Figure 44. Growth Curve Growth Rate (Gompertz Curve) QQ-Plot. Dominance model, from Mixed Linear Model GWAS test.

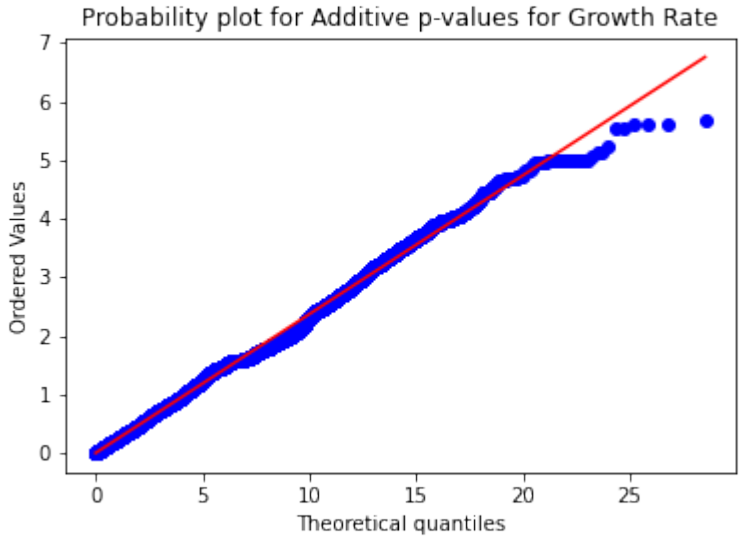

Supplementary Figure 45. Growth Curve Growth Rate (Gompertz Curve) QQ-Plot. Additive model, from Mixed Linear Model GWAS test.

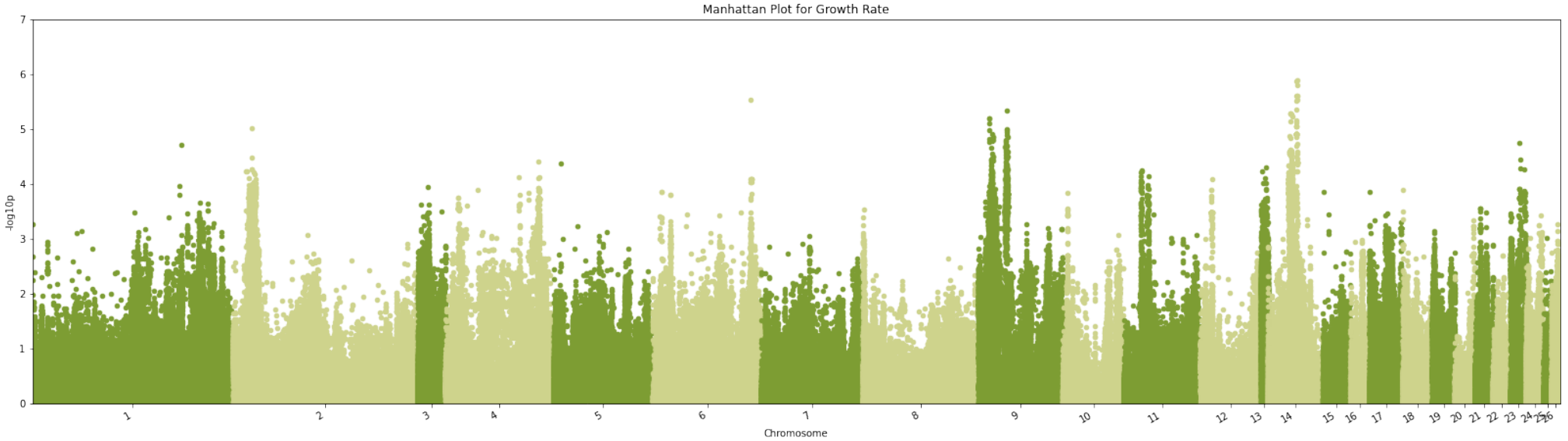

Supplementary Figure 46. Manhattan plot -log10(p) using the marker p-value from TASSEL GWAS Mixed Linear Model for Growth Curve Growth Rate for chromosomes 1 through 26 (Supplemental Table S2 for Chromosome mapping).

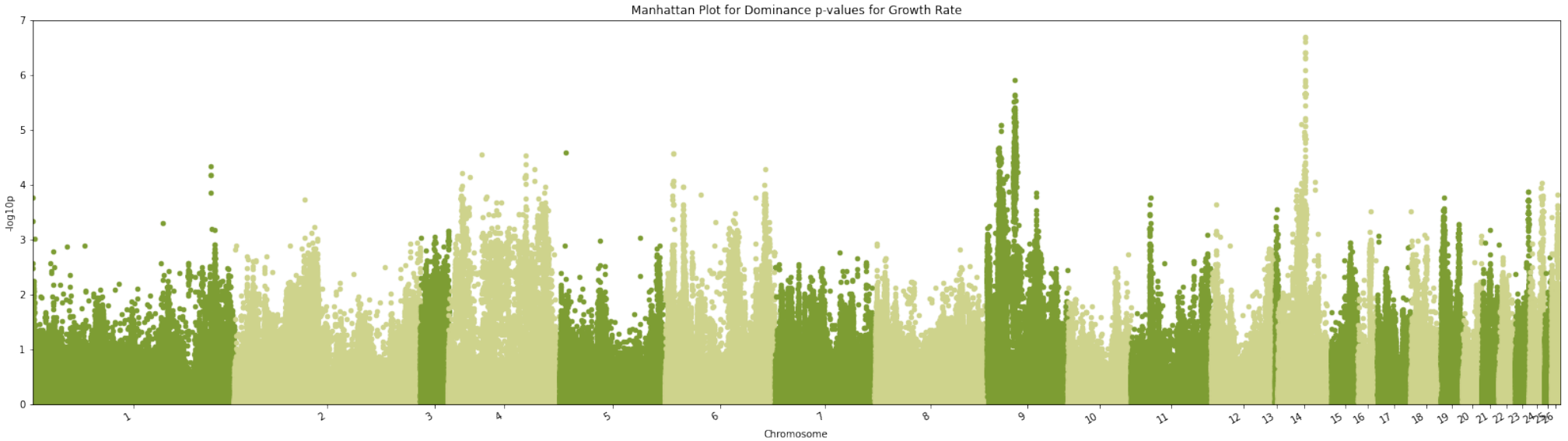

Supplementary Figure 47. Manhattan plot -log10(p) using the marker p-value from TASSEL GWAS Mixed Linear Model for Growth Curve Growth Rate for chromosomes 1 through 26 (Supplemental Table S2 for Chromosome mapping). Dominance model.

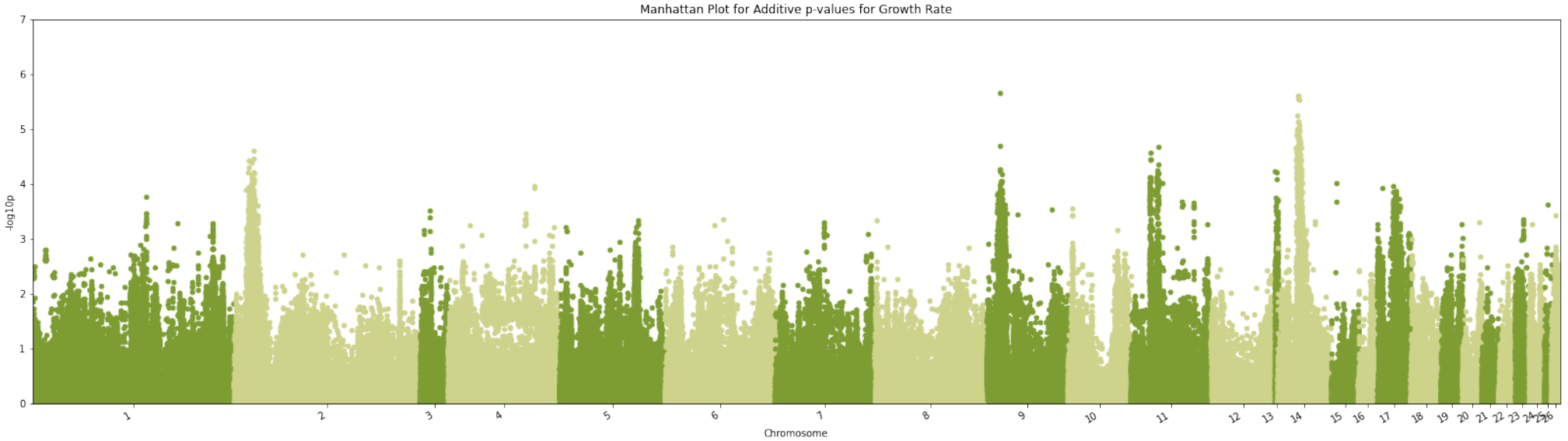

Supplementary Figure 48. Manhattan plot -log10(p) using the marker p-value from TASSEL GWAS Mixed Linear Model for Growth Curve Growth Rate for chromosomes 1 through 26 (Supplemental Table S2 for Chromosome mapping). Additive model.

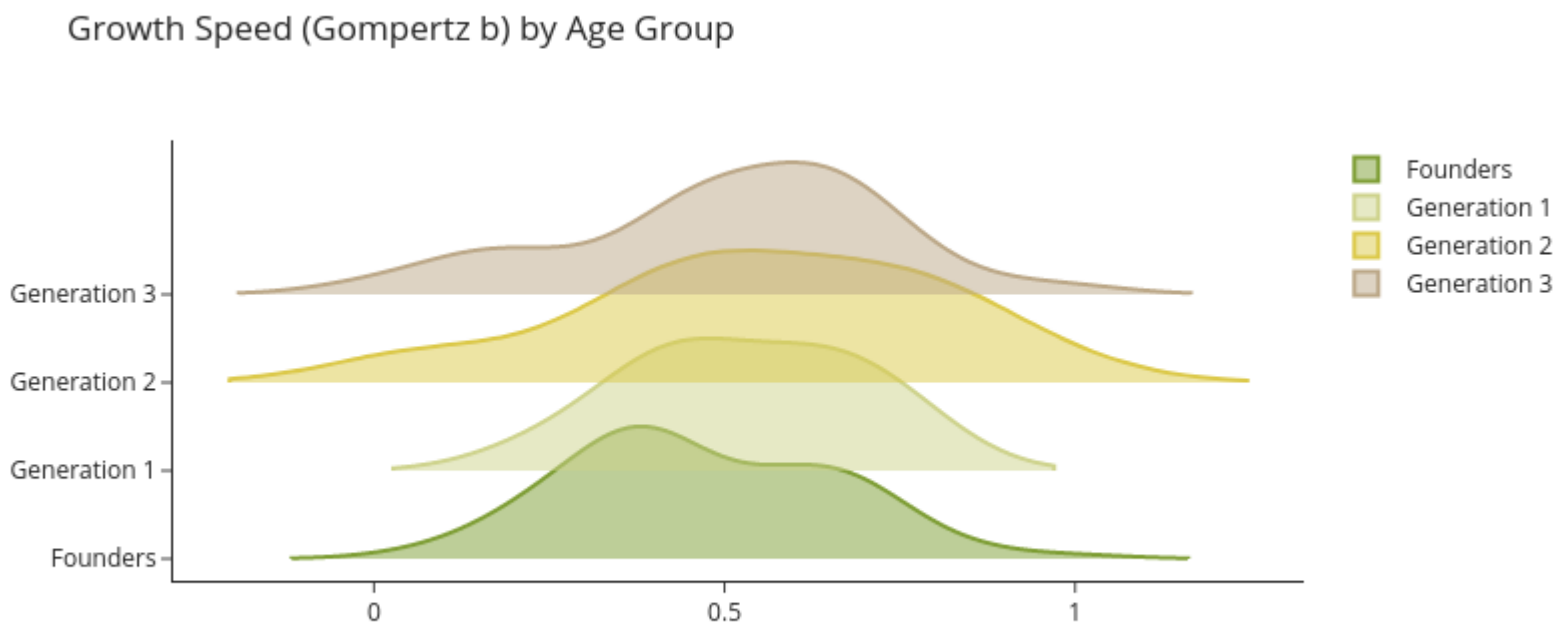

Supplementary Figure 49. Predicted Breeding Values for Growth Speed of Gompertz Curve, by generation.

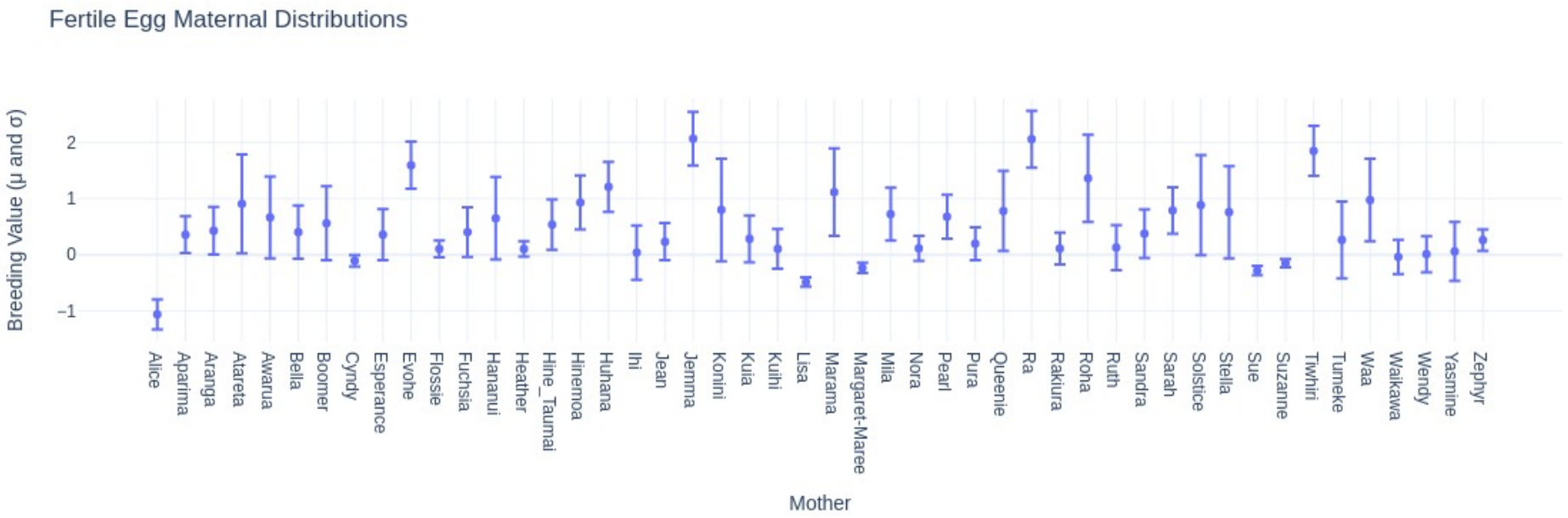

Supplementary Figure 50. Distribution of maternal effect sizes in probabilistic model. Data are presented as mean values and the standard deviation as determined by the model. n=48 maternal birds.

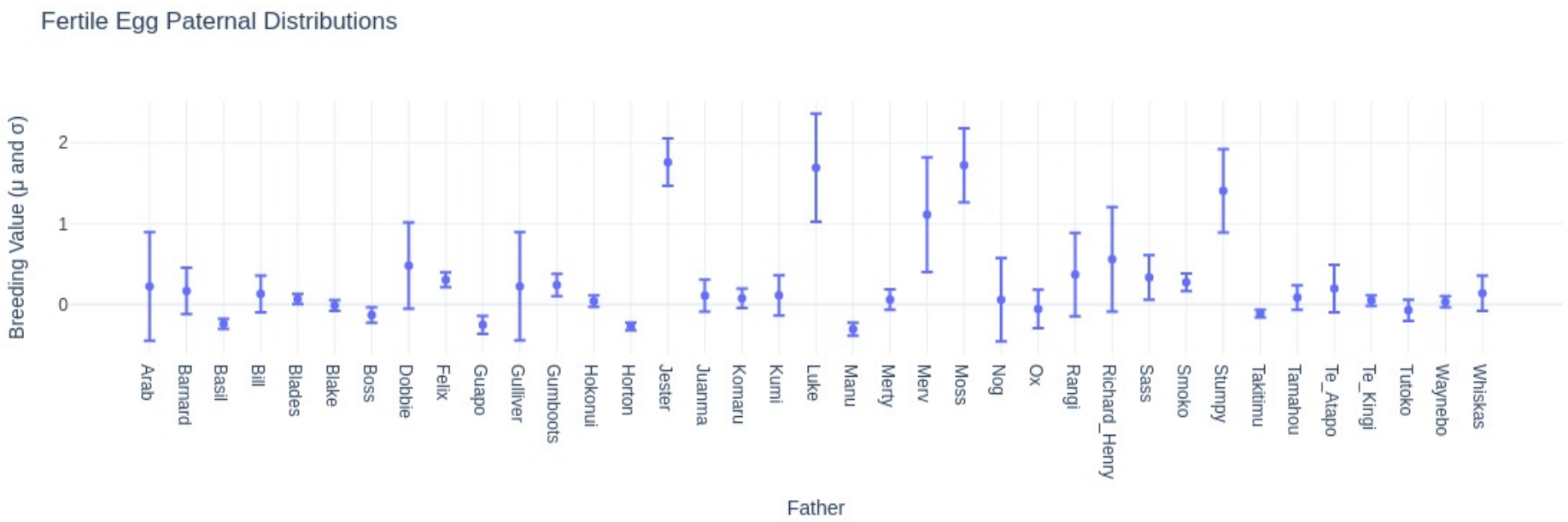

Supplementary Figure 51. Distribution of paternal effect sizes in the probabilistic model.Data are presented as mean values and the standard deviation as determined by the model. n=37 paternal birds.

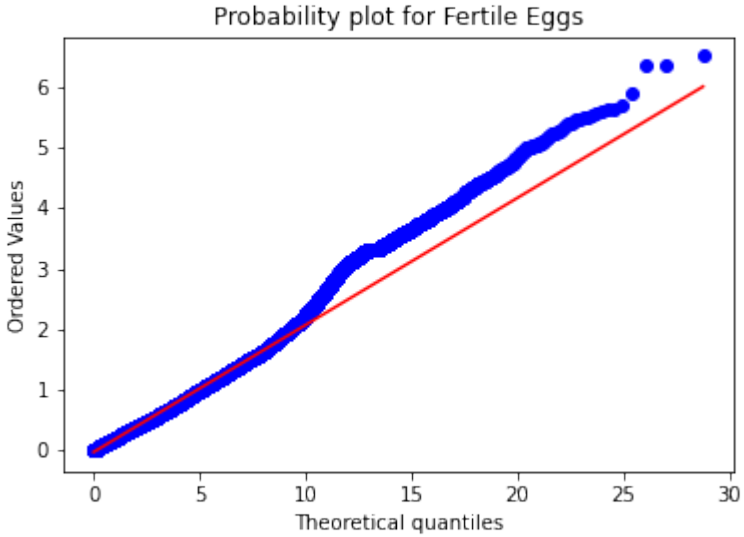

Supplementary Figure 52. QQ-Plot for Fertile Eggs GWAS, from Mixed Linear Model GWAS test.

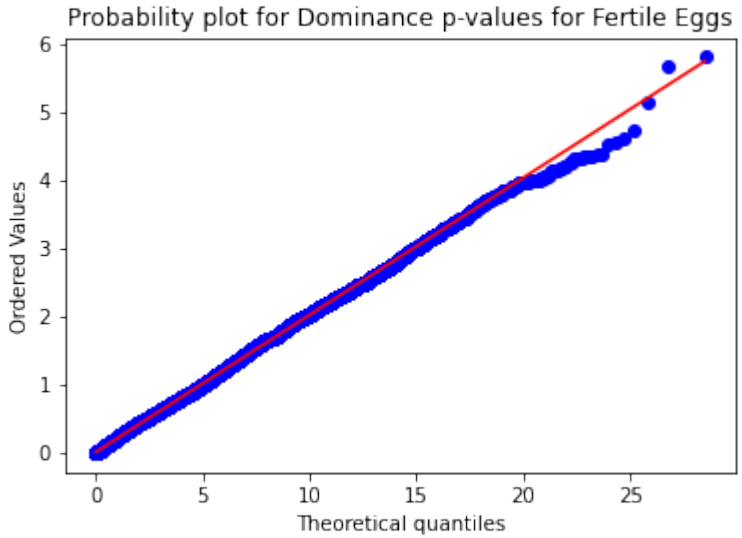

Supplementary Figure 53. QQ-Plot for Fertile Eggs GWAS. Dominance model, from Mixed Linear Model GWAS test.

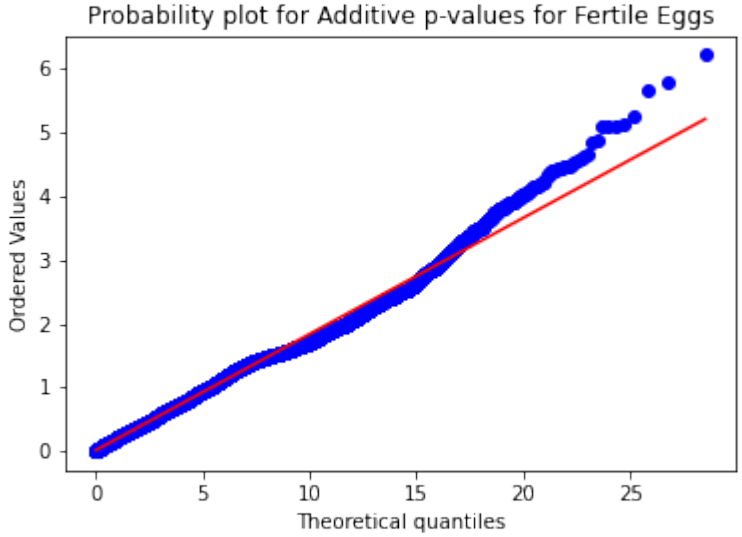

Supplementary Figure 54. QQ-Plot for Fertile Eggs GWAS. Additive model, from Mixed Linear Model GWAS test.

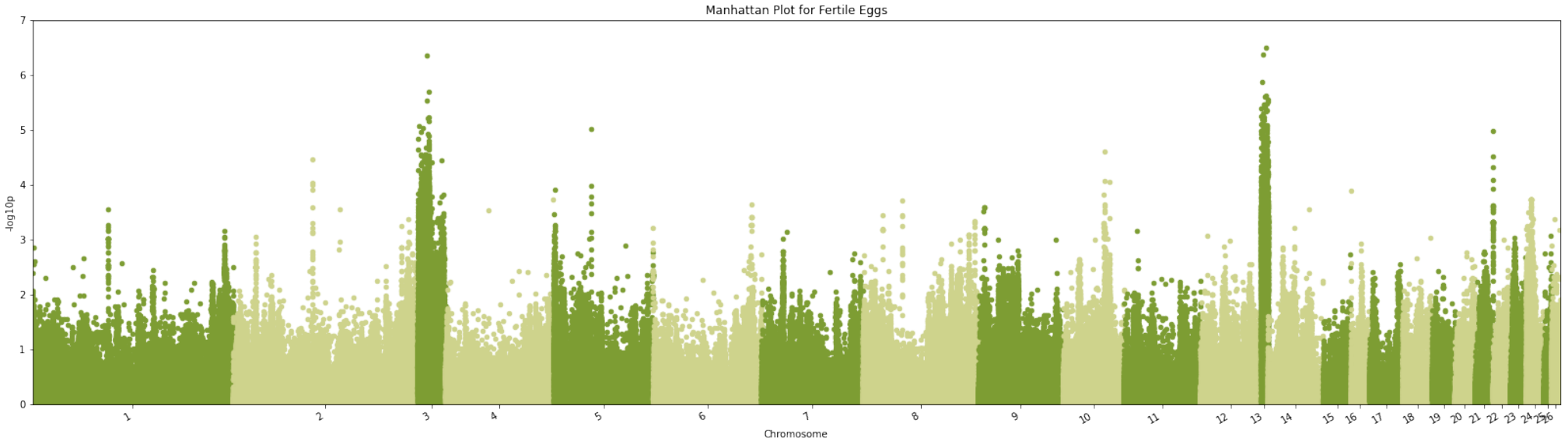

Supplementary Figure 55. Manhattan plot -log10(p) using the marker p-value from TASSEL GWAS Mixed Linear Model for Fertile Eggs for chromosomes 1 through 26 (Supplemental Table S2 for Chromosome mapping).

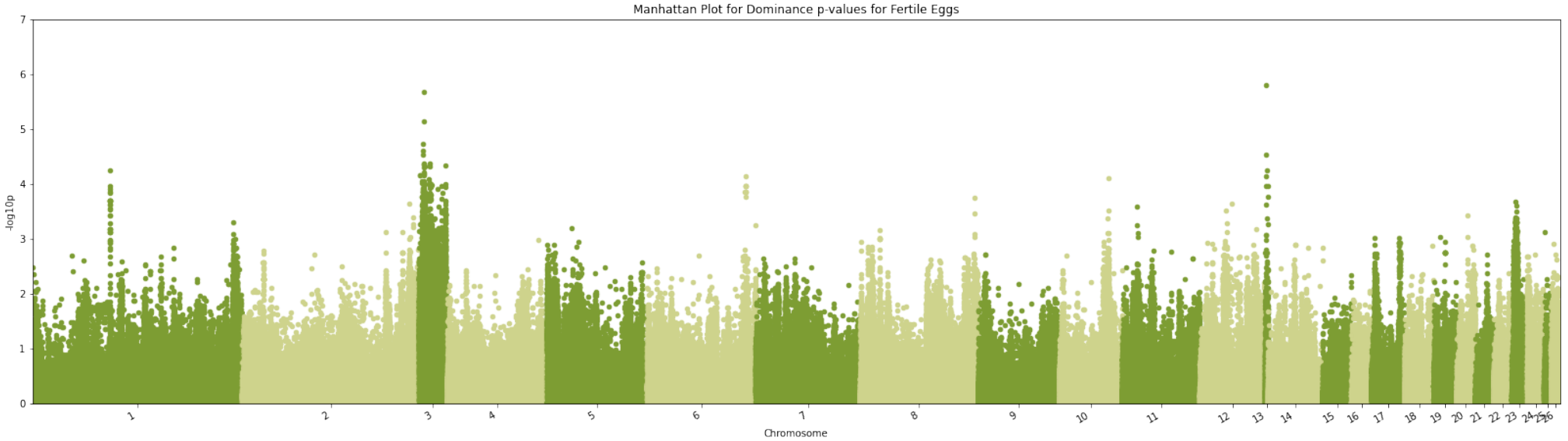

Supplementary Figure 56. Manhattan plot -log10(p) using the marker p-value from TASSEL GWAS Mixed Linear Model for Fertile Eggs for chromosomes 1 through 26 (Supplemental Table S2 for Chromosome mapping). Dominance model.

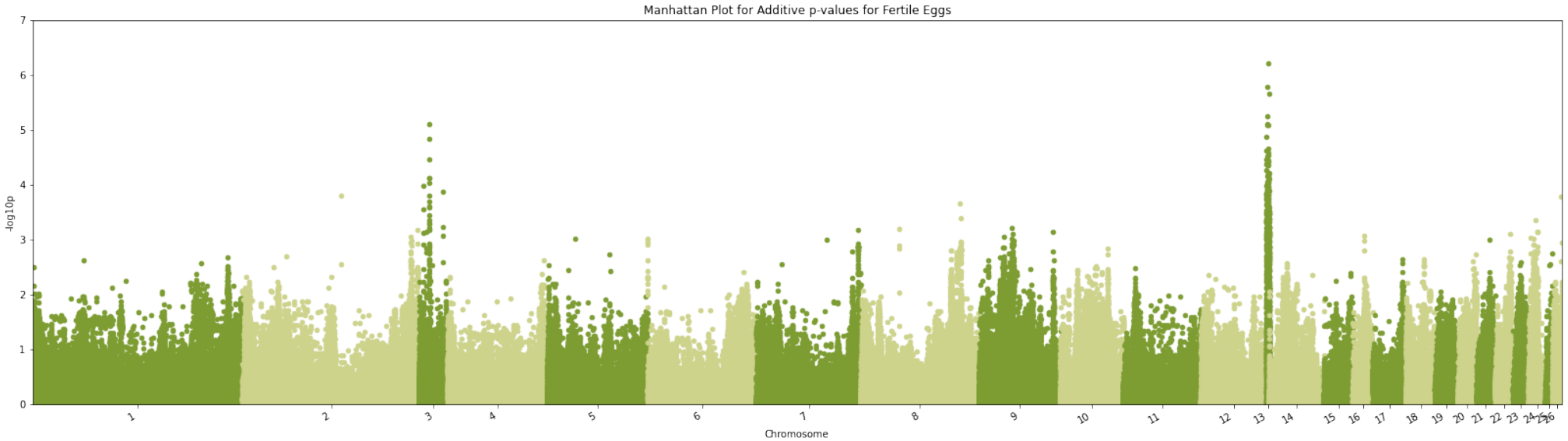

Supplementary Figure 57. Manhattan plot -log10(p) using the marker p-value from TASSEL GWAS Mixed Linear Model for Fertile Eggs for chromosomes 1 through 26 (Supplemental Table S2 for Chromosome mapping). Additive model.

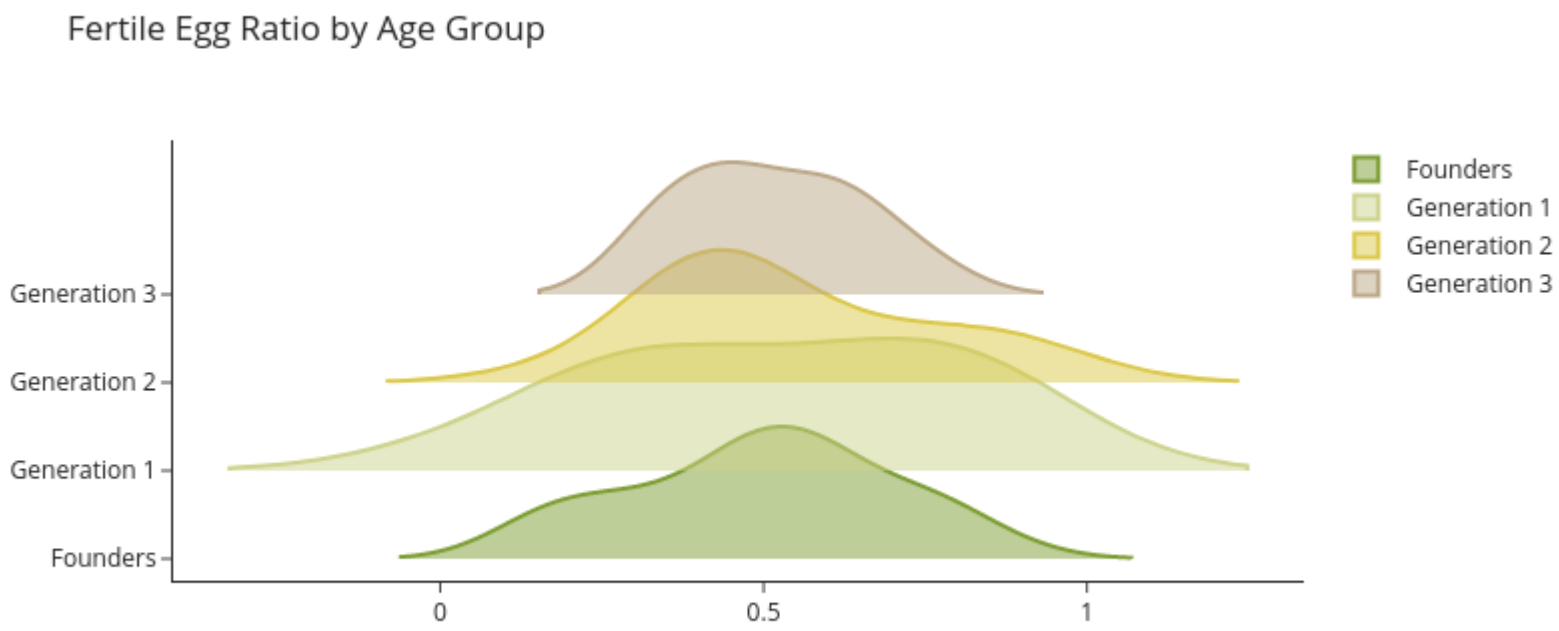

Supplementary Figure 58. Predicted breeding values for fertile eggs by age group.

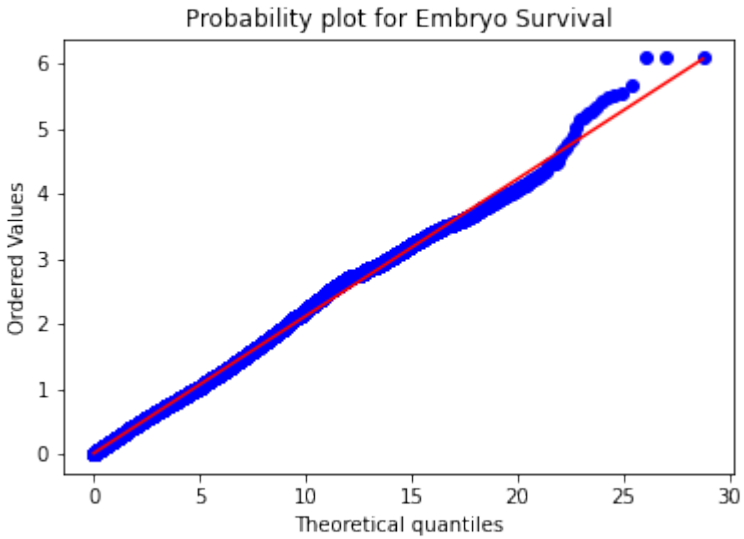

Supplementary Figure 59. QQ-Plot for Embryo Survival GWAS, from Mixed Linear Model GWAS test.

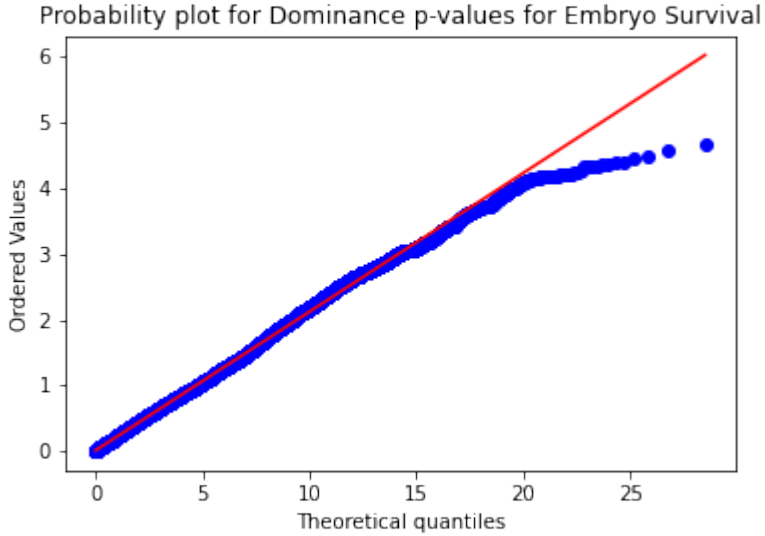

Supplementary Figure 60. QQ-Plot for Embryo Survival GWAS. Dominance model, from Mixed Linear Model GWAS test.

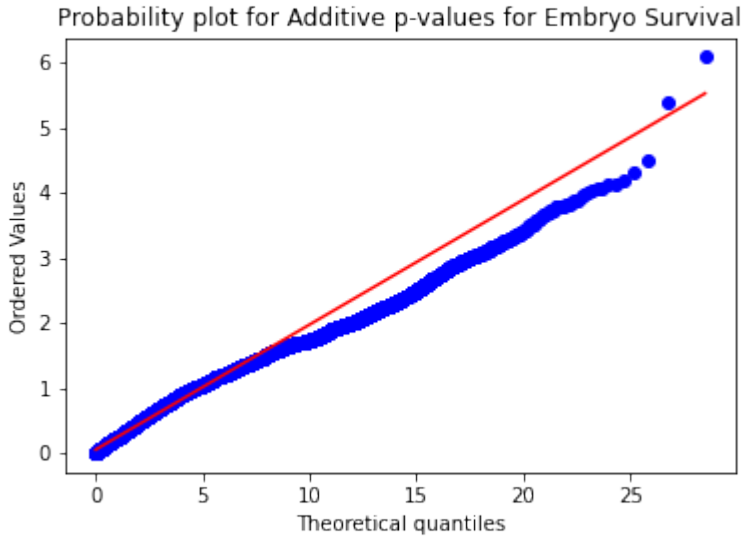

Supplementary Figure 61. QQ-Plot for Embryo Survival GWAS. Additive model, from Mixed Linear Model GWAS test.

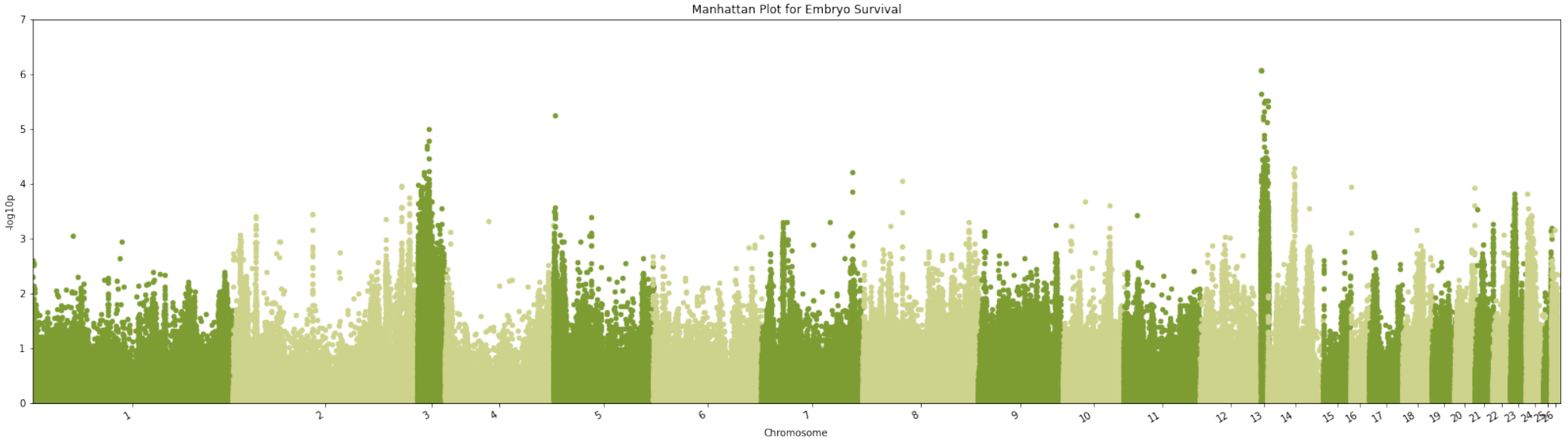

Supplementary Figure 62. Manhattan plot -log10(p) using the marker p-value from TASSEL GWAS Mixed Linear Modelfor Embryo Survival for chromosomes 1 through 26 (Supplemental Table S2 for Chromosome mapping).

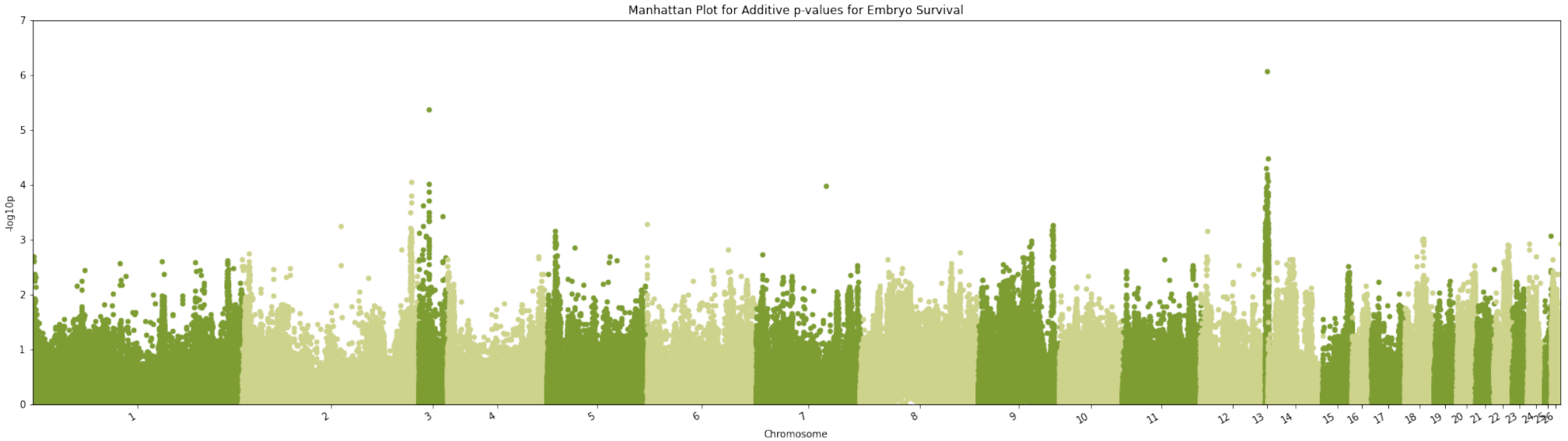

Supplementary Figure 63. Manhattan plot -log10(p) using the marker p-value from TASSEL GWAS Mixed Linear Model for Embryo Survival for chromosomes 1 through 26 (Supplemental Table S2 for Chromosome mapping). Dominance model.

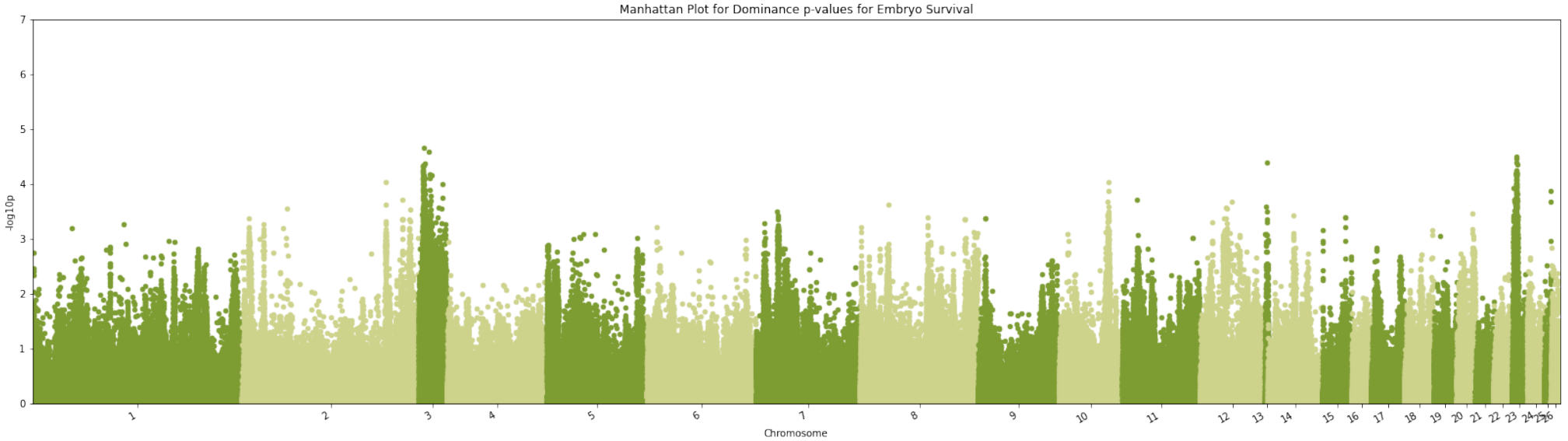

Supplementary Figure 64. Manhattan plot -log10(p) using the marker p-value from TASSEL GWAS Mixed Linear Model for Embryo Survival for chromosomes 1 through 26 (Supplemental Table S2 for Chromosome mapping). Additive model.

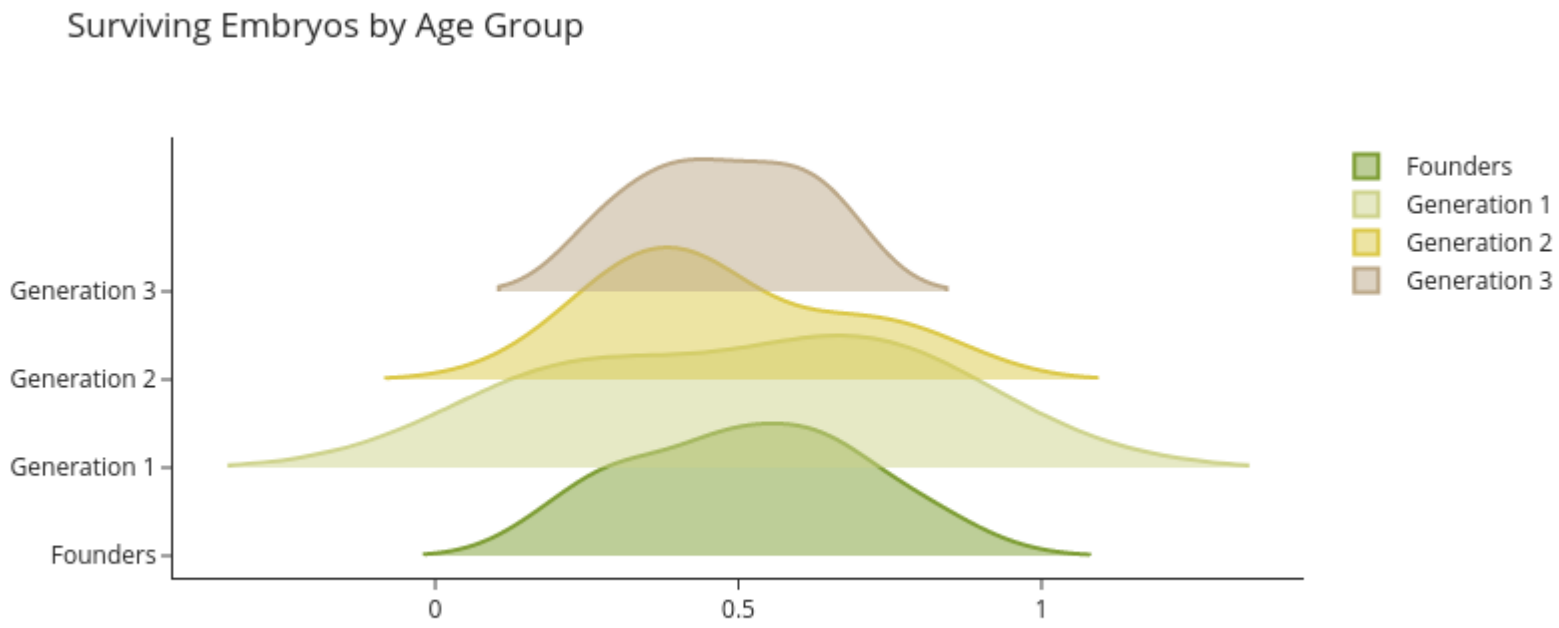

Supplementary Figure 65. Predicted breeding values for embryo survival by age group.

Supplementary Figure 66. Risk estimate predicted from model.

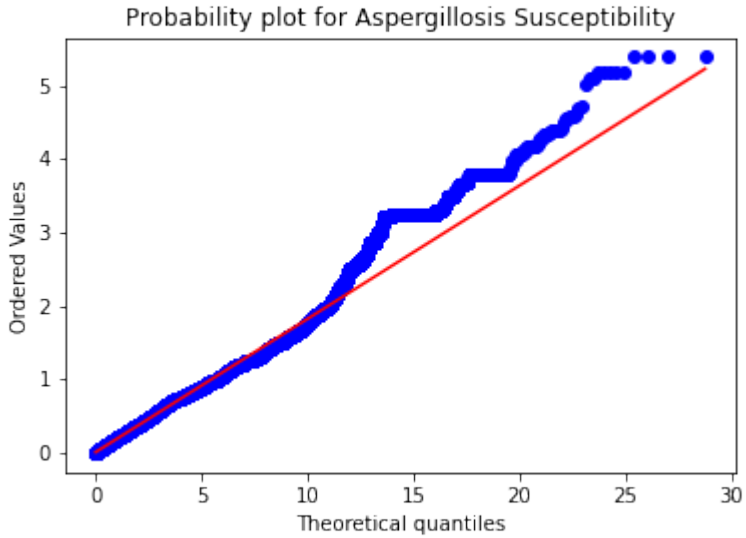

Supplementary Figure 67. QQ-Plot for Aspergillosis susceptibility, from Mixed Linear Model GWAS test.

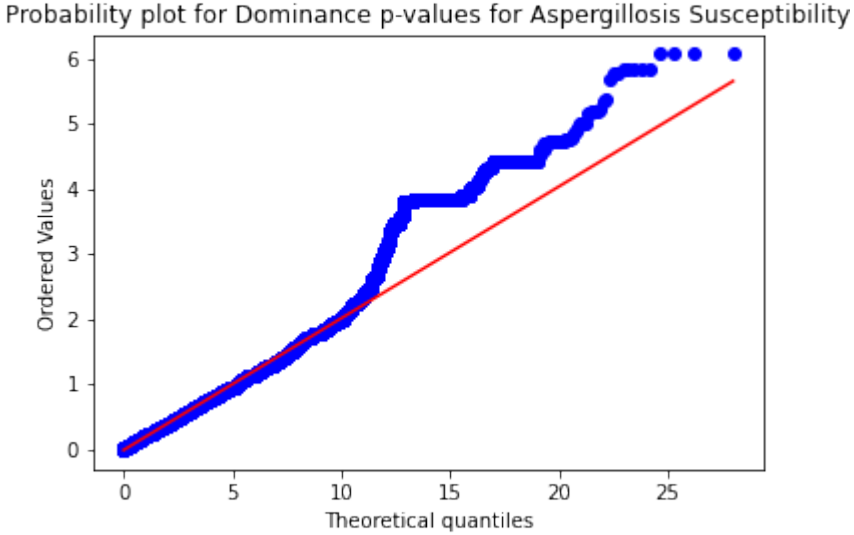

Supplementary Figure 68. QQ-Plot for Aspergillosis susceptibility. Dominance model, from Mixed Linear Model GWAS test.

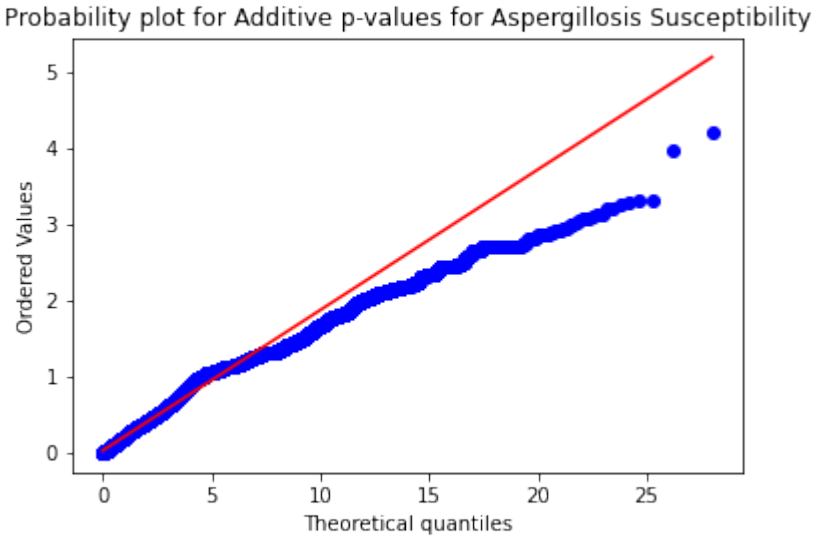

Supplementary Figure 69. QQ-Plot for Aspergillosis susceptibility. Additive model, from Mixed Linear Model GWAS test.

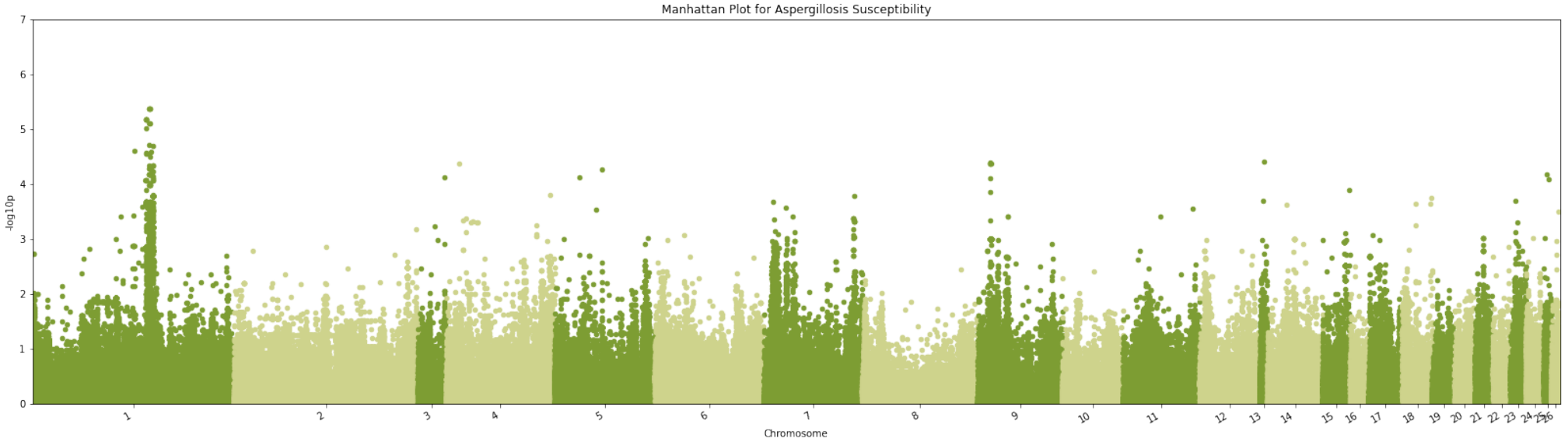

Supplementary Figure 70. Manhattan plot -log10(p) using the marker p-value from TASSEL GWAS Mixed Linear Model for Aspergillosis Susceptibility for chromosomes 1 through 26 (Supplemental Table S2 for Chromosome mapping).

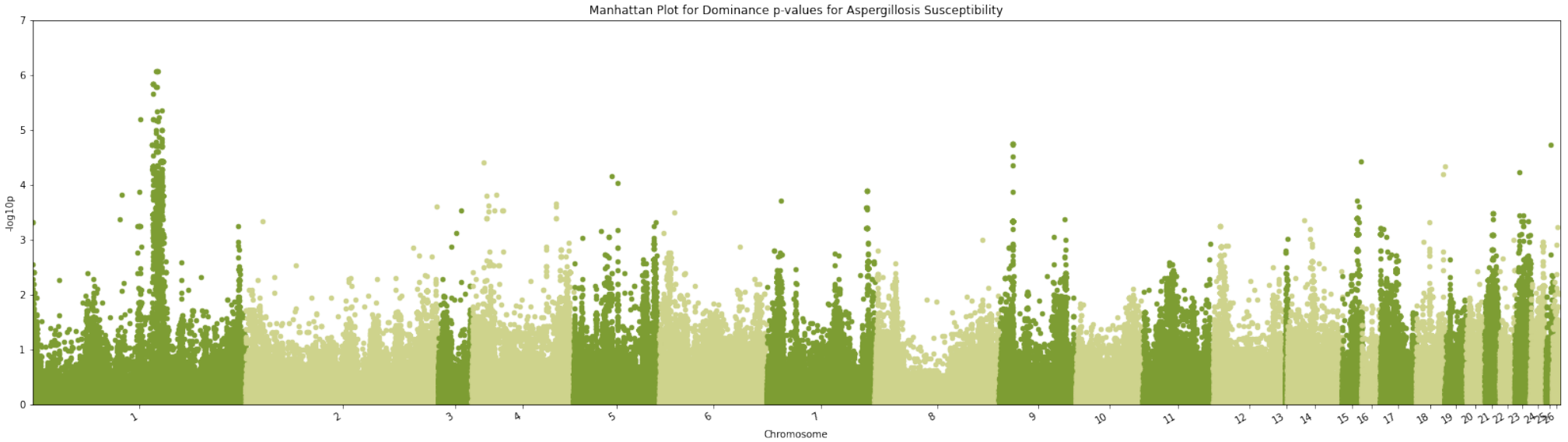

Supplementary Figure 71. Manhattan plot -log10(p) using the marker p-value from TASSEL GWAS Mixed Linear Model for Aspergillosis Susceptibility for chromosomes 1 through 26 (Supplemental Table S2 for Chromosome mapping). Dominance model.

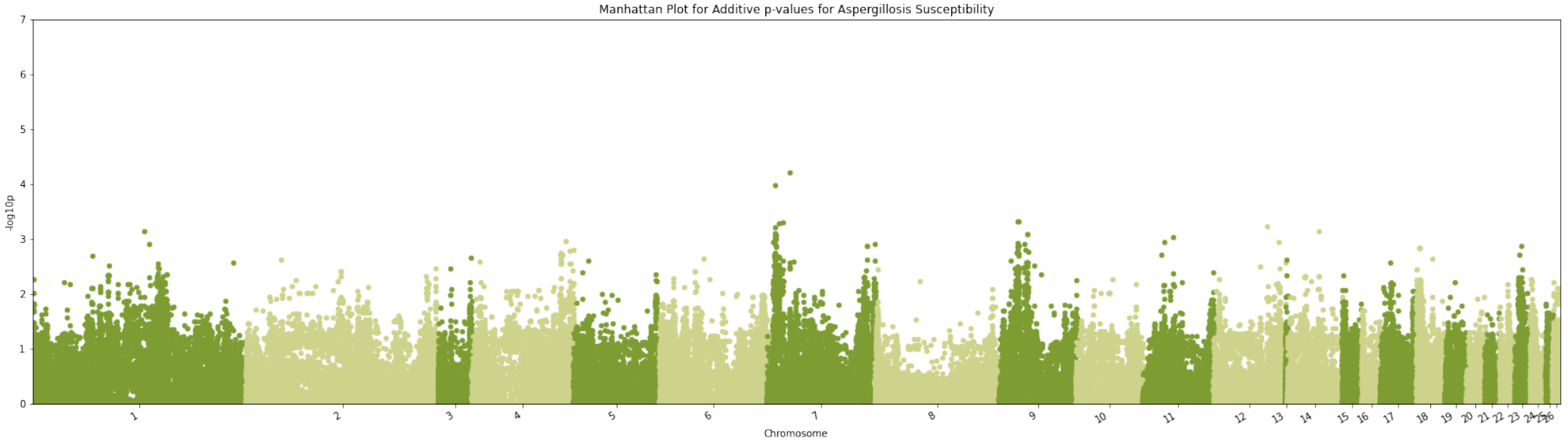

Supplementary Figure 72. Manhattan plot -log10(p) using the marker p-value from TASSEL GWAS Mixed Linear Model for Aspergillosis Susceptibility for chromosomes 1 through 26 (Supplemental Table S2 for Chromosome mapping). Additive model.

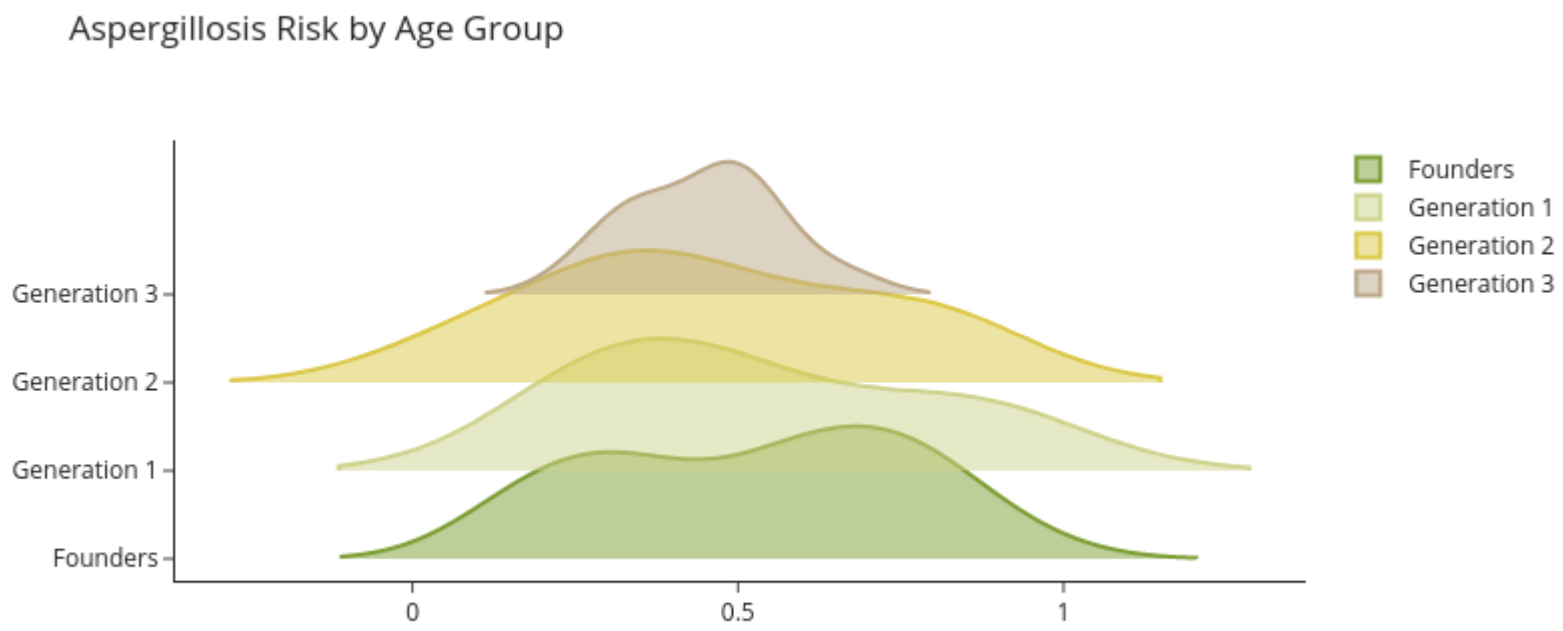

Supplementary Figure 73. Predicted breeding values for Aspergillosis risk by age group.

Supplementary Figure 74. Image of Mahli, a female kākāpō that was translocated to Te Kakahu in 2020, thanks to the genomics-informed pedigree.
Andrew Digby / New Zealand Department of Conservation